Atmospheric Research 315 (2025) 107827

Contents lists available at ScienceDirect

Atmospheric Research

journal homepage: www.elsevier.com/locate/atmosres

# A multi hazard extreme weather event in Southern Italy: Assessment and sensitivity tests of the WRF model

E. Avolio [a,*], G. Castorina [b], R.C. Torcasio [c], S. Federico [c]

[a] National Research Council of Italy, Institute of Atmospheric Sciences and Climate (CNR-ISAC), Lamezia Terme, Italy
[b] Italian Institute for Environmental Protection and Research (ISPRA) - Geological Survey of Italy Department, Rome, Italy
[c] National Research Council of Italy, Institute of Atmospheric Sciences and Climate (CNR-ISAC), Rome, Italy

ARTICLE INFO

*Keywords:*
Flood
Tornado
WRF
Data assimilation
Mediterranean
Southern Italy
Extreme weather

ABSTRACT

A deep convective system affected the southern Mediterranean on 3–4 December 2022 causing heavy rains and wind gusts over three Italian regions (Sicily, Calabria, and Apulia) and a tornado in Calabria. We study the forecast sensitivity of this multi-hazard weather event to different physical parameterizations and configuration settings of the WRF (Weather Research and Forecasting) model, used at convection permitting horizontal resolution; in particular, we performed sensitivity tests on the role of the initial and boundary conditions, on the Sea Surface Temperature (SST), on the model horizontal resolution and on the cumulus parameterization. Moreover, a 6 h rapid update data assimilation analysis (3DVAR)/forecast cycle was investigated to further study the short-term forecast capabilities of the modeling system. Most of the WRF configurations are able to well simulate the characteristics of the weather system, even if there are differences among the configurations, especially at the local scale, which causes differences in forecast performances. We found that the quality of the forecast is sensitive to the initial and boundary conditions with the best members having a probability of detection around 30–40 % for rainfall intensities of 40–50 mm/6 h. Most of the forecasts decrease their performance for larger precipitation thresholds, with few exceptions. Specifically, we found that increasing the horizontal resolution was beneficial for the case study as the probability of detection remains larger than 0.2 for rainfall thresholds larger than 60 mm/6 h and up to 100 mm/6 h. In addition, the forecast with lightning and radar reflectivity data assimilation has a probability of detection larger than 0.4 for the same intense thresholds; in both cases false alarms are not increased. For the tornado simulation, no improvement was found adopting 3DVAR. A possible forecasting strategy for severe weather events is outlined.

## 1. Introduction

This work aims to provide a scientific contribution for the better understanding and managing of an increasingly existing social and environmental issue: natural disasters in general, and extreme meteorological events in particular.

The impact of natural disasters continues to rapidly increase, fueled by the climate emergency. Several initiatives are multiplying, all over the world, aimed at improving knowledge of environmental and climate issues, as well as for the possible design of systems to manage such emergencies, to reduce disaster risks and to provide adaptation strategies to cope with the changing climate.

Over the last few years various disaster risk management (DRM) systems have been created and developed, and all have been also recognized as vitally important tools by the Intergovernmental Panel on Climate Change's (IPCC's) Sixth Assessment Report (AR6) (Calvin et al., 2023). Among them, the recently developed multi-hazard early warning systems (MHEWS) (UNDRR, 2023) deserve mention. This system, like other similar ones, aims to address several hazards and/or impacts of similar or different types in contexts where extreme events may occur alone, simultaneously, or cascading. A multi-warning system considers a multitude of different components (e.g., preparedness and awareness; observation and monitoring; warning dissemination and communication) but it cannot be done without a forecasting component to produce useful alerts.

It is by following this direction that we are addressing the issue of refining a meteorological modeling system able to correctly predict not only a specific weather event, but also a possible coexistence of multiple

* Corresponding author.
*E-mail address:* e.avolio@isac.cnr.it (E. Avolio).

https://doi.org/10.1016/j.atmosres.2024.107827
Received 21 June 2024; Received in revised form 26 November 2024; Accepted 27 November 2024
Available online 30 November 2024

extreme meteorological phenomena.

Natural disasters and extreme weather events might occur in all parts of the world, including the Mediterranean area, which is considered a climate "hotspot" due to its high sensitivity to climate variability and change (Giorgi, 2006). The Mediterranean is particularly prone to severe weather events. The main forcings are to be found in the warm sea and in the complex orography; the synoptic-scale meteorology often triggers extreme weather phenomena of different nature, whose forecast is one of the major missions to cope for the forecaster community.

In this work we study a deep convective system in the southern Mediterranean that affected three Italian regions (Sicily, Calabria and Apulia) on 3–4 December 2022 producing heavy rains, floods, wind gusts and a tornado.

Severe weather phenomena are not uncommon in this area, and several works discussed the capabilities of numerical weather prediction models at the mesoscale for a wide range of extreme events.

Sicily region, mainly during the autumn period, and particularly the eastern sector, is often affected by intense weather events (e.g., Forestieri et al., 2018; Aronica et al., 2012; Caccamo et al., 2017). A more recent event hit the region, with heavy and high localized rainfall, on 15 July 2020; this case was studied by Federico et al. (2021), that also evaluated the impact of radar reflectivity and lightning data assimilation on the RAMS (Regional Atmospheric Modeling System) model forecast, and by Castorina et al. (2022), who studied the role of the grid resolution in the prediction of the event. Castorina et al. (2023) also investigated the performance of the WRF model in forecasting a V-Shaped Storm hitting Sicily on 11–12 November 2019.

Calabria region has been affected by several flood events over the years; in particular, they deserve to be mentioned the well-known "Crotone flood", "Soverato flood" and "Vibo Valentia flood" (Federico et al., 2003a, 2003b; Gascón et al., 2016). A more recent work of Avolio and Federico (2018) can be considered as a reference also for the results achieved in this work. In that case, the authors studied a severe convective event that hit central-eastern Calabria, between 30 Oct - 02 Nov, 2015, evaluating the sensitivity of the quantitative precipitation forecast (QPF) to different physical parameterization schemes and configuration settings of the WRF model. Finally, another sadly well-known event (causing 10 casualties), namely the "Raganello flood" (20 August 2018), was studied in Avolio et al. (2019) that provided a hydro-meteorological analysis of the event evaluating the forecasting skills of a modeling system based on the WRF-WRF-Hydro models.

Regarding the Apulia region, Miglietta and Regano (2008) studied a flash-flood episode affecting a small area on 22 October 2005 to understand the mechanisms responsible for the heavy rain event. Mastrangelo et al. (2011) performed high resolution simulations for a heavy precipitation event that affected the Ionian areas of Basilicata and Apulia during 12 and 13 November 2004, revealing the presence of two intense localized convective systems.

In addition to floods, other interesting extreme weather events affecting the Mediterranean and southern Italy regions, which are attracting growing interest over recent years, are tornadoes. Considering studies mainly focused on severe tornadoes able to cause significant damages in the Mediterranean, Miglietta and Rotunno (2016) and Miglietta et al. (2017a and 2017b) studied in detail an EF3 tornado occurred in southeastern Italy. More recently, Avolio and Miglietta (2021) carried out a modeling study on four tornado-spawning supercells over southern Italy, hitting the same (Ionian) regions and characterized by common synoptic conditions.

Several authors adopted multi-physics ensemble approaches to evaluate the role/impact of the different parameterization schemes in WRF for various weather phenomena. Sofokleous et al. (2021) proposed a combination of 18 atmospheric physics parameterizations for the WRF model, to study the precipitation field over a small and topographically complex area in the Mediterranean (Cyprus Island). Stegehuis et al. (2015) conducted a study performing a large combination of different atmospheric physics schemes (216 simulations) to study two European mega heat waves. Ricchi et al. (2019) evaluated the skill of a multi-physics ensemble (18 combinations with WRF model) for the simulation of a tropical-like cyclone in the Mediterranean Sea. From these studies, it follows that there is no single configuration that is suitable for all events and/or for all areas; for this reason, new types of approaches, both physical and statistical, are taking hold to refine the model capabilities.

Most of the case studies considered in the papers cited above, as well as the case study analyzed in this paper, involve deep convection at the least in some stages of the storm. These events are very difficult to predict because of their large variation in space and time and because of the multitude of physical processes involved in convective storms (Stensrud et al., 2009).

A possible way to cope with these events is through rapid update analysis/forecast cycles (RUC) with data assimilation at the local scale (Benjamin et al., 2004). This approach was used in several parts of the world with the aim of issuing alerts for severe weather or deep convective events. In many studies the radar reflectivity and/or lightning are used in the assimilation process. Focusing over Italy, Federico et al. (2017, 2019) showed the importance of a RUC cycle assimilating lightning and/or radar reflectivity for short-term (3 h) prediction of deep convective events. Further analyses were performed in this direction by Torcasio et al. (2020, 2023a) and Mazzarella et al. (2022), showing that lightning data assimilation is very important to forecast events at the local scale with high spatio-temporal precision and can be easily implemented in RUC cycle (Mansell et al., 2007; Fierro et al., 2012). Other studies involving radar reflectivity data assimilation (Gastaldo et al., 2021; Maiello et al., 2017; Mazzarella et al., 2020) showed a positive and substantial improvement of precipitation forecast of convective events, especially at the short-range ($< 6$ h). In few of these studies it was also shown that the impact of data assimilation was larger when convection is forced and developed at the local scale compared to cases when the large-scale forcing brings the instability that is consumed by convection, which are more predictable (Keil et al., 2014).

The positive impact of data assimilation on the precipitation forecast of deep convective events was also shown for GNSS-ZTD data (Faccani et al., 2005; Lagasio et al., 2019; Torcasio et al., 2023b), with or without the assimilation of other sources of data, for rainfall data (Davolio et al., 2017; Torcasio et al., 2024) and for the assimilation of surface weather stations (Maggioni et al., 2023). In all these studies, it was concluded that data assimilation is a powerful tool to refine the numerical weather prediction as the storm is approaching or occurring.

This work aims to conduct a modeling study on an extreme convective system characterized by multiple meteorological hazards, aiming at defining a possible strategy to improve severe weather forecasts. Specifically, the strategy is a two-step process: first, to run a model ensemble at moderate-high horizontal resolution to define the possibility of occurrence of a severe weather event; second, to run a RUC assimilating local observations that can improve the forecast of the event more precisely while the storm is approaching or occurring. To complete the analysis, we run a set of sensitivity tests to evaluate the impact of some important parameters (Sea Surface Temperature and horizontal resolution) on the event forecast. These tests can be conducted post-event to find better configuration for future applications. To our knowledge, no work on similar events, or with these objectives/modalities, has yet been conducted in the area here studied.

The paper is organized as follows. Section 2 describes the available observations, the statistics used to evaluate the model performance and the WRF model configuration strategies. Section 3 firstly describes the case study and the main meteorological conditions during the event, then reports the main results about the simulation of the heavy rainfall and the tornado. Section 4 provides a summary and the conclusions.

## 2. Data and methods

### 2.1. Observations

This section provides a short description of the dataset used in the work. Several types of data are considered: CAPPI (Constant Altitude Plan Position Indicator) of radar reflectivity, raingauges, lightning, and weather reports data are used for the analysis of the event and for the verification of the forecast; lightning and radar reflectivity data are also used for data assimilation. The available radar reflectivity maps (composite reflectivity, provided by the Italian Department of Civil Protection, DCP hereafter) are used for the event description, while radar CAPPI of the national radar composite at 2000 m, 3000 m, 4000 m,5000 m, 6000 m, 7000 m and 8000 m, are assimilated.

To verify the precipitation forecast and to study the characteristics of the event we used a subset of raingauges of the Italian network. This network is composed of more than 4000 raingauges belonging to the Italian regions and centralized by the DCP. As we focus on southern Italy, we use about 1000 out of the 4000 raingauges. The distribution of the raingauges is rather homogeneous over Southern Italy, as shown in Fig. 1b.

Flashes are clear indicators of deep convection and are provided by the LINET network (LIghtning NETwork, Betz et al., 2009), which is a ground-based network operating in the LF/VLF range. The network has more than 200 sensors over Europe, where it has the highest Detection Efficiency (DE). A recent analysis of the characteristics of the LINET network over Italy and of the lightning recorded in the last 13-years is reported in Petracca et al. (2024), showing a good DE (>95 %) of the LINET network over the area considered in this study.

The growing interest in severe meteorological phenomena led to an increasing popularity of groups / citizen science's projects / websites devoted to archive and record weather events, often including photos and videos. For some phenomena, as for tornadoes, the visual reporting is the unique opportunity to assess the events; moreover, only a post-event investigation allows the classification (e.g., Enhanced Fujita scale, for tornadoes) of the phenomena. In this study, in addition to the available measurements, a tornado occurred in Calabria is also investigated by consulting the report collected by the public Storm Report database, managed by PRETEMP (www.pretemp.it; De Martin et al., 2023) and Meteonetwork association (Giazzi et al., 2022), a group of professional meteorologists, amateurs and students.

### 2.2. Model configuration and simulations' schemes

All the simulations are performed using the fully compressible, non-hydrostatic WRF-ARW (Weather Research and Forecasting Advanced Research WRF) model (Skamarock et al., 2019) version 4.3.

Two two-way nested domains are used (Fig. 1a); the parent domain covers the Italian peninsula (10 km grid spacing; 146 × 146 grid points), while the inner domain covers southern Italy (2 km grid spacing; 281 × 296 grid points). For a WRF sensitivity test (see below) we slightly changed the domains to double up the horizontal resolution, namely using a nested domain covering a similar area in southern Italy, with 1 km grid spacing and 400 × 400 grid points. The model is employed with 40 terrain-following vertical levels.

Two datasets are considered for the initial and boundary conditions (IC/BC): NCEP-GFS (National Center for Environmental Prediction - Global Forecast System) analysis/forecast fields (0.25° horizontal resolution), and ECMWF-IFS (European Centre for Medium-Range Weather Forecasts - Integrated Forecasting System) fields (0.1° horizontal

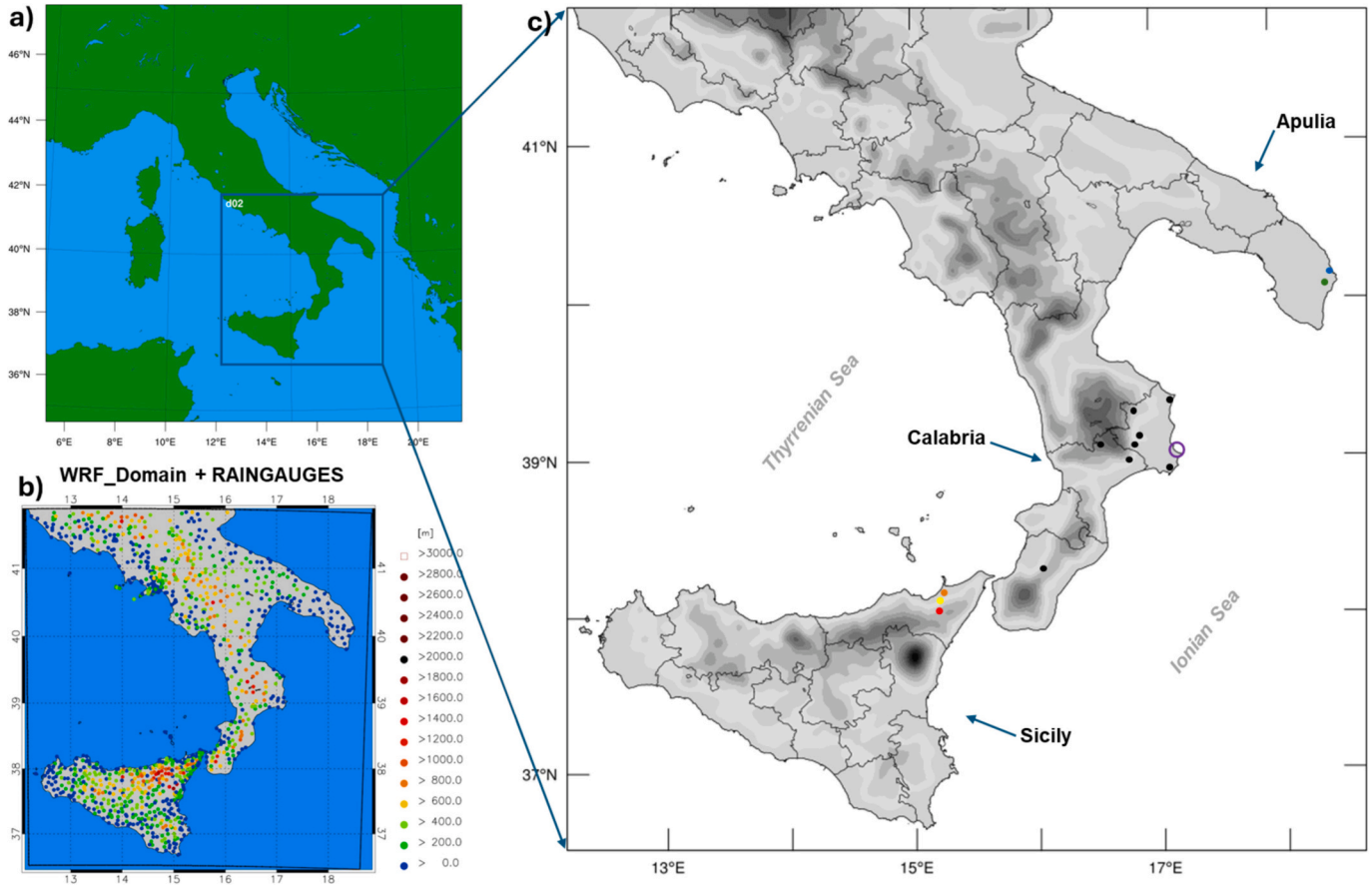


**Fig. 1.** (a) WRF domains; (b) the raingauges adopted for the model verification; (c) the 2 km spacing WRF model inner domain and terrain height (m); some locations cited in the text are also shown in this panel c.

resolution).

Each simulation starts at 06 UTC, on 3 December and lasts 30 h, with the first 6 h considered as spin-up. Thus, the verification-period goes from 12 UTC, 3 December, to 12 UTC, 4 December (24 h).

For each IC/BC dataset 18 runs are carried out, combining:

- 3 microphysics schemes: i) WRF Single-Moment 6-class (WSM6) (Hong and Lim, 2006; Dudhia et al., 2008); ii) Thompson (Thompson et al., 2008); iii) WRF single moment 7-class (WSM7) (Bae et al., 2019).
- 3 planetary boundary layer (PBL) schemes: i) Yonsei University (YSU) (Hong et al., 2006); ii) Mellor–Yamada–Janjic (MYJ) (Janjić, 1994); iii) Asymmetrical Convective Model version 2 (ACM2) (Pleim, 2007).
- 2 cumulus parameterization schemes: i) Betts–Miller–Janjić (BMJ) (Betts and Miller, 1986); ii) Kain–Fritsch (KF) (Kain, 2004). Convection is explicitly resolved for the fine grid, except for one sensitivity test.

The new Rapid Radiative Transfer Model (RRTMG) long-wave and short-wave radiation scheme (Iacono et al., 2000) and the Unified Noah land-surface model (Tewari et al., 2004) are used in all simulations. The parameterization schemes here adopted were chosen based on our experience in using the WRF model for the simulation of extreme events in the area. In fact, the proposed schemes have already been widely used in previous works and have shown their validity in terms of forecasting performance. As regards the microphysics schemes, in particular, our experience so far has always led us to successfully use single-moment schemes (e.g., Avolio and Miglietta, 2022; Avolio and Federico, 2018; Torcasio et al., 2023a; Federico et al., 2024). However, we recognize the high potential of using double-moment schemes and we intend, in future works aimed at testing this proposed methodology, to adopt them to verify their effectiveness.

Combining all the schemes and the two IC/BC datasets, a total of 36 runs are performed.

The 36 runs are compared with rain gauges observations to identify the best configuration. Once the best configuration is found, 3 further sensitivity tests are conducted using the same physical parameterization of the best configuration, in order to assess: i) the role of convection (activating the cumulus parameterization scheme also for the innermost domain); ii) the possible role of SST (replacing the initial SST field, taken from the ECMWF-IFS, with the observed "Multi-Scale Ultra High Resolution" SST (MUR; JPL MUR MEaSUREs Project, 2015); iii) the role of adopting a higher horizontal resolution (performing a 1 km horizontal resolution WRF simulation). The horizontal resolution falls within the well-known gray zone of convection, and the role of cumulus parameterization, at these resolutions, is still an open question in the modeling community (Hong et al., 2012). Several studies have assessed that the explicit treatment of convection using high resolution grid spacings led to considerable improvements (e.g., Richard et al., 2007; Schwartz et al., 2009; Weusthoff et al., 2010); at the same time, other works (e.g., Wagner et al., 2018; Gimhan et al., 2023) showed how the activation of cumulus schemes, also at high resolution (1–3 km), produced valuable results for the precipitation forecast and for simulation of extreme rainfall events. Aware of this, the first sensitivity test was still done to see if, by parameterizing also the unresolved part of the convection, improvements could be obtained for the prediction of strongly convective events like the one studied here.

Finally, a data assimilation experiment is performed. In this test lightning and CAPPI of radar reflectivity from 2 km to 8 km every 1 km are assimilated. Data assimilation is performed following this scheme: the first six hours of each simulation are the spin-up, then follows the 3DVAR, and finally a 6 h forecast. With this forecast configuration four simulations are needed to cover the whole period. The 3DVAR scheme used is that of Federico (2013), recently adapted to the WRF model (Torcasio et al., 2023a). For each assimilation time (00, 06, 12, 18), flashes observed in the former 30 min are used, while CAPPI of radar reflectivity are available at the assimilation time. In the 3DVAR, the atmospheric columns where lightning is observed are saturated between the Lifting Condensation Level (LCL; computed from the background) and the −25 °C isotherm. CAPPIs of radar reflectivity are assimilated following the scheme of Wang et al. (2013). Radar data assimilation is performed only where/when the radar reflectivity is above 15dBZ and the vertically integrated liquid water content is above 1.5 mm. These thresholds are applied to avoid, at least partially, the generation of spurious convection, which is the main drawback of lightning and radar reflectivity data assimilation (Federico et al., 2019; Torcasio et al., 2023a). Considering the scheme used for assimilating radar reflectivity and lightning, two variables are taken into account: the water vapor for both lightning and radar data assimilation, and rain mixing ratios for radar data assimilation.

The background error matrix is simply prescribed: to maintain the data assimilation at the local scale, the horizontal error de-correlation length-scale is 15 km, while the vertical decorrelation length scale is 500 m. The observation error matrix is diagonal. The observation error for the water vapor mixing ratio decreases with height, starting from the 3 g/kg value at the surface. The observation error for the rain mixing ratio is 1 g/kg. The background error at each level is twice the observation error to give more credit to observations than to the model.

Before data assimilation, the CAPPIs of radar reflectivity are superobbed at 5 km horizontal resolution starting from the initial 1 km horizontal resolution. This operation reduces the amount of data for the assimilation and partially accounts for neglecting the observation error spatial correlations.

### 2.3. Verification methods

To assess the model performance for rainfall prediction, we compute both dichotomous categorical scores and quantitative metrics. The precipitation forecast is verified for time intervals of 6 h starting at 12 UTC on 3 December and ending at 12 UTC on 4 December to show the model performance in the different phases of the storm. For categorical scores, the contingency tables are built considering 51 precipitation thresholds: 1 mm/6 h and from 2 mm/6 h up to 100 mm/6 h every 2 mm/6 h.

Starting from the hits (A), false alarms (B), misses (C), and correct no forecasts (D), we compute: the probability of detection (POD; range [0,1], where 1 is the perfect score), the False Alarm Rate (FAR; range [0, 1], where 0 is the perfect score), and the equitable threat score (ETS; range [−1/3,1], where 1 is the perfect score and 0 is a useless forecast) (Wilks, 2006).

They are calculated as:

$$\mathrm{POD} = \mathrm{A}/(\mathrm{A}+\mathrm{C}).$$

$$\mathrm{FAR} = \mathrm{B}/(\mathrm{A}+\mathrm{B}).$$

$$\mathrm{ETS} = (\mathrm{A}-\mathrm{Er})/(\mathrm{A}+\mathrm{C}+\mathrm{B}-\mathrm{Er}).$$

where Er is:

$$\mathrm{Er} = [(\mathrm{A}+\mathrm{B})^{*}(\mathrm{A}+\mathrm{C})]/(\mathrm{A}+\mathrm{B}+\mathrm{C}+\mathrm{D}).$$

Quantitative metrics (standard deviations, root mean squared error and correlation coefficient, between forecasts and observations) are also computed for time intervals of 6 h and represented by the Taylor diagram (Taylor, 2001). The Taylor diagram graphically summarizes how closely a pattern matches observations. The similarity between two patterns (forecast and observed 6 h precipitation) is quantified in terms of their correlation, their centered root mean square differences, and their standard deviations (amplitude of variations). To limit the uncertainties related to a possible point-by-point comparison, due to the high resolution of the WRF domain, the statistical verification, between WRF outputs and measurements, is carried out by means of the "best nearest neighbor" approach, considering the four model grid points nearby the location of each rain gauge and selecting the one exhibiting the closest value to the observation. Furthermore, to consider the shape

and the structure of the precipitation pattern, we also reported the results in terms of rain maps (Section 3.2). Anyway, verification based on dichotomous categorical scores might suffer from the well-known problem of double penalty error (Wilks, 2006). To account for this issue, the performance is also quantified using the Fractions Skill Scores (FSS, Roberts and Lean, 2008), which is well suited for evaluating forecasts produced by neighborhood approaches; results for FSS analysis are shown in Appendix A.

## 3. Results and discussion

### 3.1. Case description

The identification of the main phases of the event and the related phenomena was achieved thanks to i) the available radar composite reflectivity images; ii) the lightning maps; iii) the reports provided by PRETEMP; iv) the precipitation recorded by raingauges.

Figure 2 shows two radar maps (panels a,b) and the IR10.8 μm channel satellite image from Meteosat-8 (panel c), which refer to the two main phases of the event (12 UTC on 03 December and 00 UTC on 04 December, respectively).

A convective system affected three southern Italy regions (Sicily, Calabria, and Apulia; see Fig. 1c) on 3–4 December 2022. In its north-eastern motion, the perturbed system firstly affected Sicily causing thunderstorms on the north-eastern side of the region (Fig. 2a), where highly localized and heavy rainfall caused flooding and landslides.

During the night between 3 and 4 December the system reached the eastern side of the Calabria region (Fig. 2b), causing very intense rainfall; flooding and traffic disruption have been documented in the area. Embedded within the convective system, an EF2 (Enhanced Fujita scale, EF hereafter; Doswell et al., 2009) tornado affected Isola Capo Rizzuto, in eastern Calabria (see Fig. 1c). On the morning of 4 December, the system moved towards Apulia, before dissolving, causing moderate rain and wind gusts, as reported by PRETEMP.

A typical V-shaped signature is recognizable from the radar images and from the IR satellite image (Fig. 2c). This structure, not uncommon for extreme meteorological events in southern Italy (e.g., Castorina et al., 2023; Avolio and Miglietta, 2021), is mainly associated with overshooting cloud-top and intense storm updrafts (Setvák et al., 2010) and is a clear indication of severe convection (Brunner et al., 2007).

Considering the rainfall during the whole event (from 12 UTC on 3 December to 12 UTC on 4 December), and the rainfall recorded by the weather stations of the DCP (Fig. 3), the rain gauge of Novara (see the red dot in Fig. 1c), in northeastern Sicily, recorded the maximum amount of precipitation (> 300 mm / 24 h), as well as other two stations registered rainfall >200 mm / 24 h (Rodì and Barcelona P. G.; see yellow

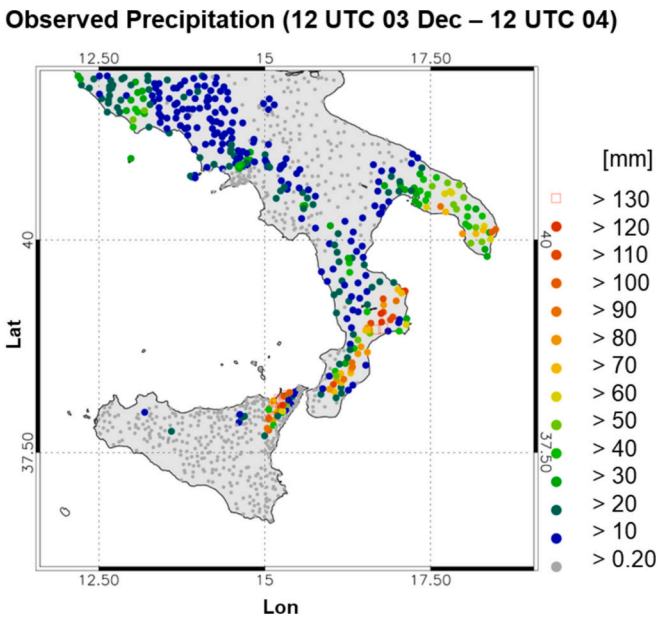


**Fig. 3.** Rainfall (mm) recorded by the weather stations of the DCP between 12 UTC on 3 December 2022 and 12 UTC on 04 December 2022.

and orange dots in Fig. 1c); twelve rain gauges recorded rainfall >130 mm / 24 h in the northeastern part of the region, showing the severity of the rainfall over this area. High rainfall accumulations were also recorded in Calabria, where several stations measured precipitation above 100 mm / 24 h (Cirò Marina, Savelli, Cotronei, Petronà, S.Mauro Marchesato, Albi, Molochio; see black dots on Fig. 1c). Finally, precipitation above 100 mm was also recorded by two stations in Apulia (Otranto and Minervino di Lecce; see light blue and green dots on Fig. 1c).

The maps of lightning recorded on 03 and 04 December 2022 are reported in Fig. 4 showing that the development of the storm was characterized by deep convection, as several thousand flashes occurred during the event. The flashes on the 3 December clearly reveal the convection over Northern Sicily in the afternoon and evening. The storm moved towards NE in the following hours, impacting Calabria and Apulia. This continued during the first hours of 4 December, while the storm didn't impact Sicily on that day (Fig. 4b).

As stated, the meteorological phenomena caused by this convective system are essentially: i) extreme rainfall (including hail, according with PRETEMP reports) and ii) a tornado. In the next sections we will address

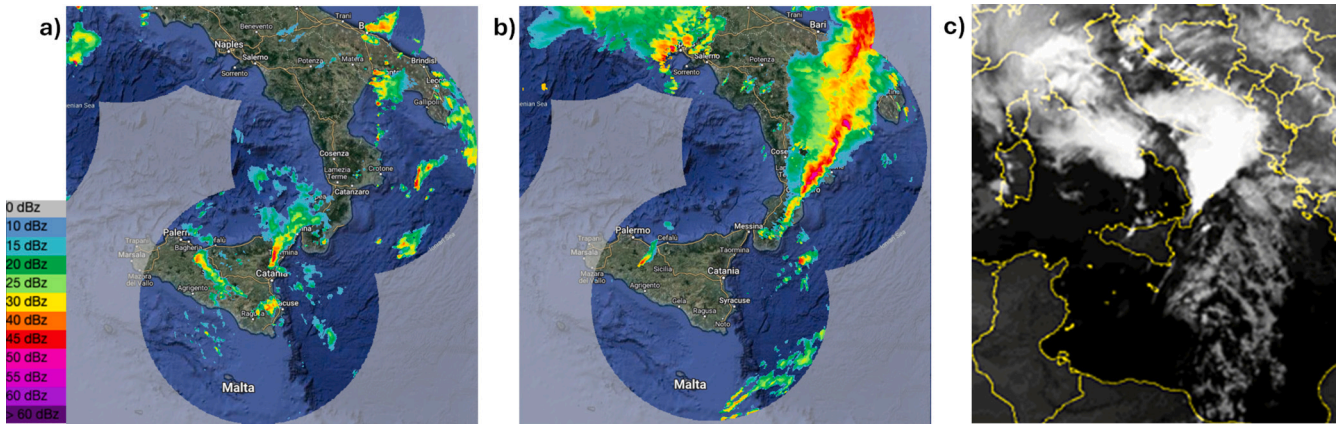


**Fig. 2.** (a) Composite radar reflectivity (dBZ) at 12 UTC, 03 December 2022 and (b) 00 UTC, 04 December 2022 (b); (c) IR10.8 μm channel satellite image from Meteosat-8 at 00 UTC, 04 December 2022. The maps in (a) and (b) are derived by the automatic system "Dewetra" of the Italian Department of Civil Protection, http://www.mydewetra.org); the map in (c) is derived by www.sat24.com (©Eumetsat).

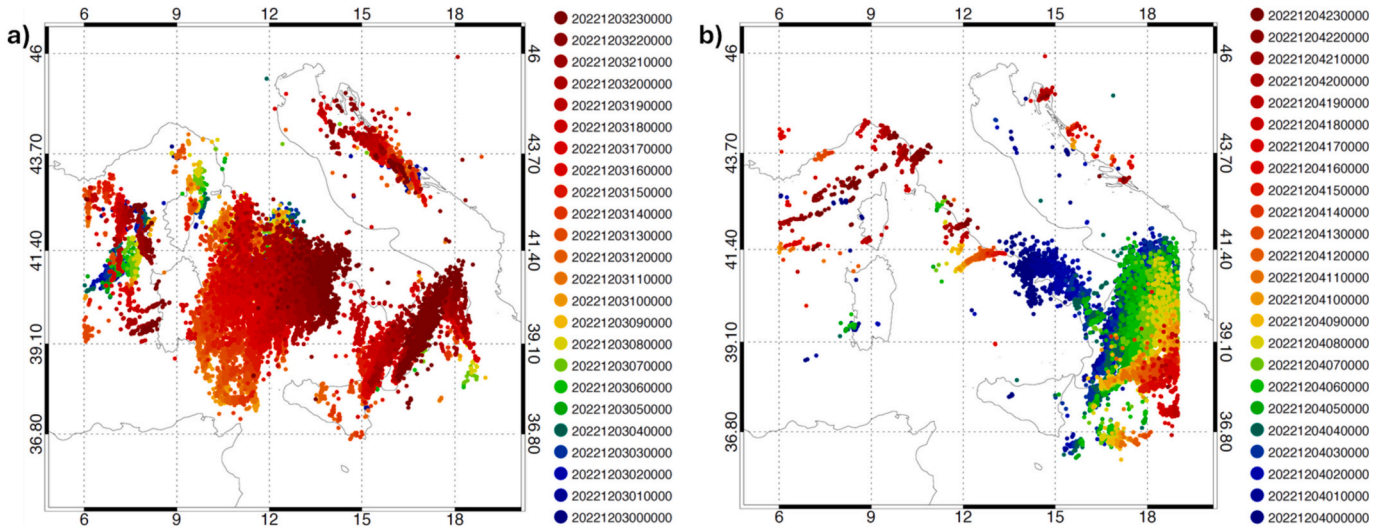


**Fig. 4.** Lightning recorded on (a) 03 and (b) 04 December 2022 over Italy and surrounding areas.

these two phenomena discussing the forecasting capabilities of the WRF-based modeling system.

### 3.2. Synoptic/mesoscale analysis

In order to analyze the synoptic conditions during the event we show, in Fig. 5, the maps of geopotential heights and winds at 500 hPa

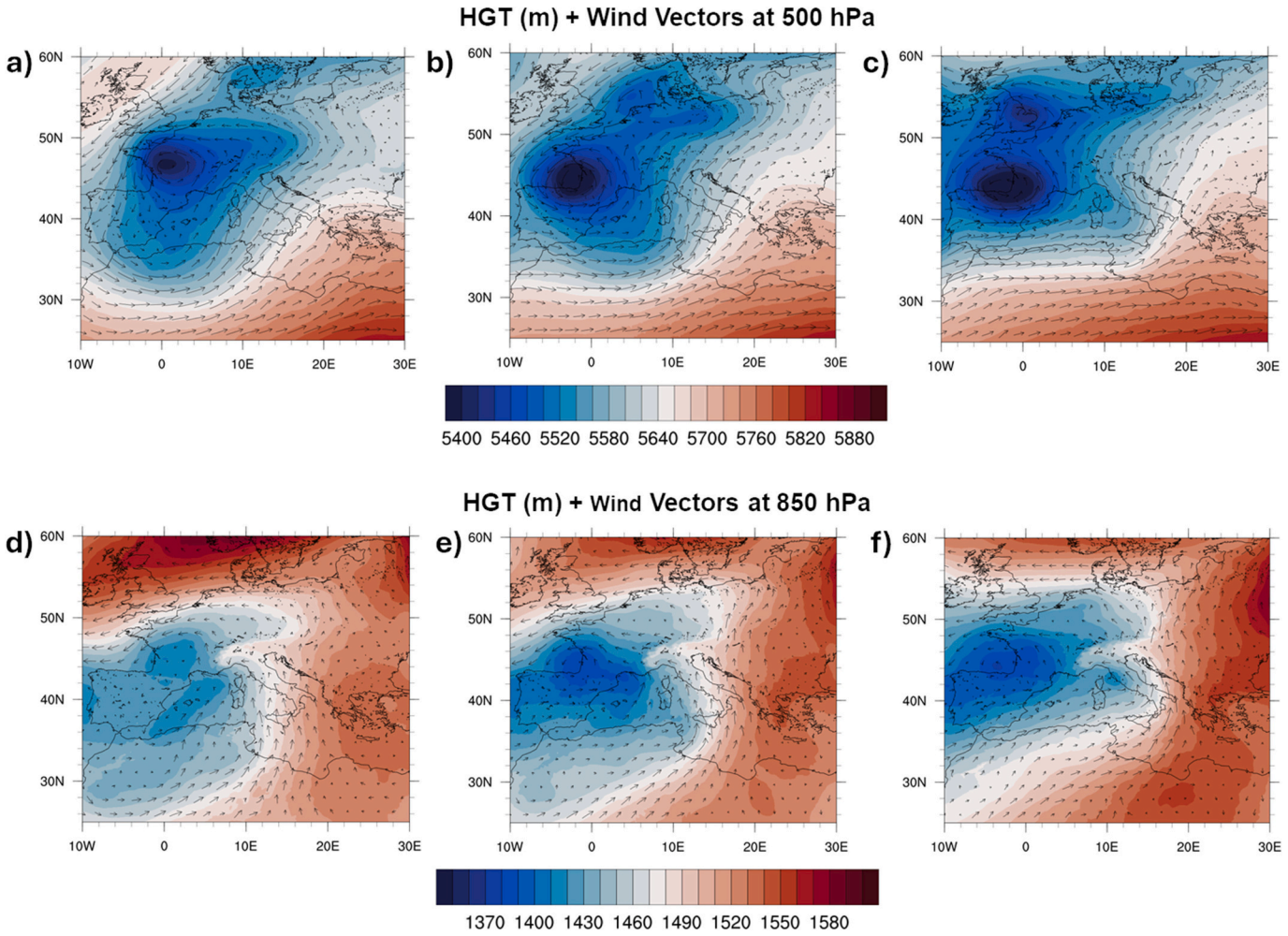


**Fig. 5.** Geopotential height (m) and wind vectors (m/s) at 500 hPa (top panels) and 850 hPa (bottom panels) at (a,d) 00 UTC, 03 December 2022; (b,e) 12 UTC, 03 December 2022, and (c,f) 00 UTC 04 December 2022.

(upper panels) and 850 hPa (bottom panels) derived from the ECMWF-IFS operational dataset, the same used as IC/BC conditions for some WRF runs. In the hours preceding the development of the severe weather event over southern Italy, the atmospheric conditions were characterized by an upper- (and mid-) level trough over western Europe, and by a wide high-pressure area over eastern Europe. The cyclonic circulation was first centered over France (Fig. 5a and d) and, in the next 24 h, it exhibited a progressive deepening and slow descent towards Spain (Fig. 5c and f). These conditions favored a persistent flowing of air masses from SW-S to NE-N, accompanied by the advection of (low-layers) warm and moist air over southern Italy, as shown by the maps of temperature at 850 hPa and specific humidity at 700 hPa (Fig. 6a and b, respectively); the former permits to highlight the presence of warm unstable air flowing from Libya and directed towards the Ionian Sea, while the latter shows the flowing of humid currents towards southern Italy regions affected by the event.

Observing the maps at different levels, it is also easily identifiable a directional wind shear between 850 and 500 hPa (we will also discuss the wind shear in section 3.3, describing the tornado that affected eastern Calabria), a precondition that generally favors unstable conditions. A further confirmation of this comes from the analysis of the radiosoundings (not shown) at Trapani (Sicily) and Galatina (Apulia) which show, as the altitude increases, a clockwise rotation of wind over southern Italy.

### 3.3. Rainfall forecast

#### 3.3.1. Scores and best run identification

One of the principal goals for this study is to assess the WRF performances for the precipitation forecast, as rainfall was the main-impacting meteorological phenomenon for the case study.

As anticipated, 36 runs were performed with different WRF configurations and IC/BC conditions. The statistics introduced in the previous section are used to identify the model configuration that better simulates the observed events. Both categorical scores and quantitative statistical parameters are computed, analyzing the scores for 6 h and other time horizons (e.g., 12 h, 24 h; not shown for brevity) for all thresholds. Fig. 7 shows ETS and POD scores for the 6 h forecasts to better follow the storm evolution. The performance is reasonable for low thresholds (20 mm / 6 h) while the scores decrease for most WRF configurations as rainfall thresholds increase. However, few runs exhibit higher ETS and POD values for thresholds greater than 50 mm / 6 h; all these runs are initialized with IFS fields, demonstrating a greater effectiveness of such IC/BC conditions for this case study. The selection of the best-performing configuration was conducted by analyzing the scores for 6 h, as well as by (qualitatively) comparing the precipitation patterns for all runs. The result of these multiple checks led to identifying the simulation named "IFS15" as the best-performing run.

This is confirmed by the analysis of the Taylor diagram reported in Fig. 8, that quantifies the similarity between the simulated rainfall patterns and the observed one in terms of their correlations, centered root-mean-square differences and standard deviations. Different runs are represented by different symbols. As regards the 36 runs varying for different IC/BC and parameterizations, the 18 simulations initialized by GFS are represented by triangles, while the 18 simulations initialized by IFS are represented by squares. Among these runs, only IFS15 is colored, while the other runs are displayed in gray. The performance of each run is inversely proportional to the distance between its symbol and the reference point (marked as "Observed", the point 1.0 on the x-axis). It is easy to see that the simulations initialized with IFS give better performance overall, in agreement with previous findings; among them, the run that shows a shorter distance than the observed field is those named IFS15, which adopts the following schemes: WSM7 for microphysics, KF for convection and YSU for PBL. The following discussion is based on IFS15, hereafter also named CTL.

In Fig. 9 we show the maximum reflectivity (a and b panel) simulated by WRF (CTL run), at the times corresponding to the main phases of the event, i.e., at 12 UTC on 3 December (a) and 00 UTC on 4 December (b), respectively. The corresponding observed reflectivities are shown in Fig. 2a and b.

During the first phase we see a good agreement between the WRF simulation and the observed pattern. It is well apparent the highly localized local maxima of reflectivity (both observed and simulated; locally >45 dBz) over northeastern Sicily, corresponding to the highest recorded rainfall of this storm. During the second phase of the event, when the system reaches Calabria, we see a well-simulated narrow area

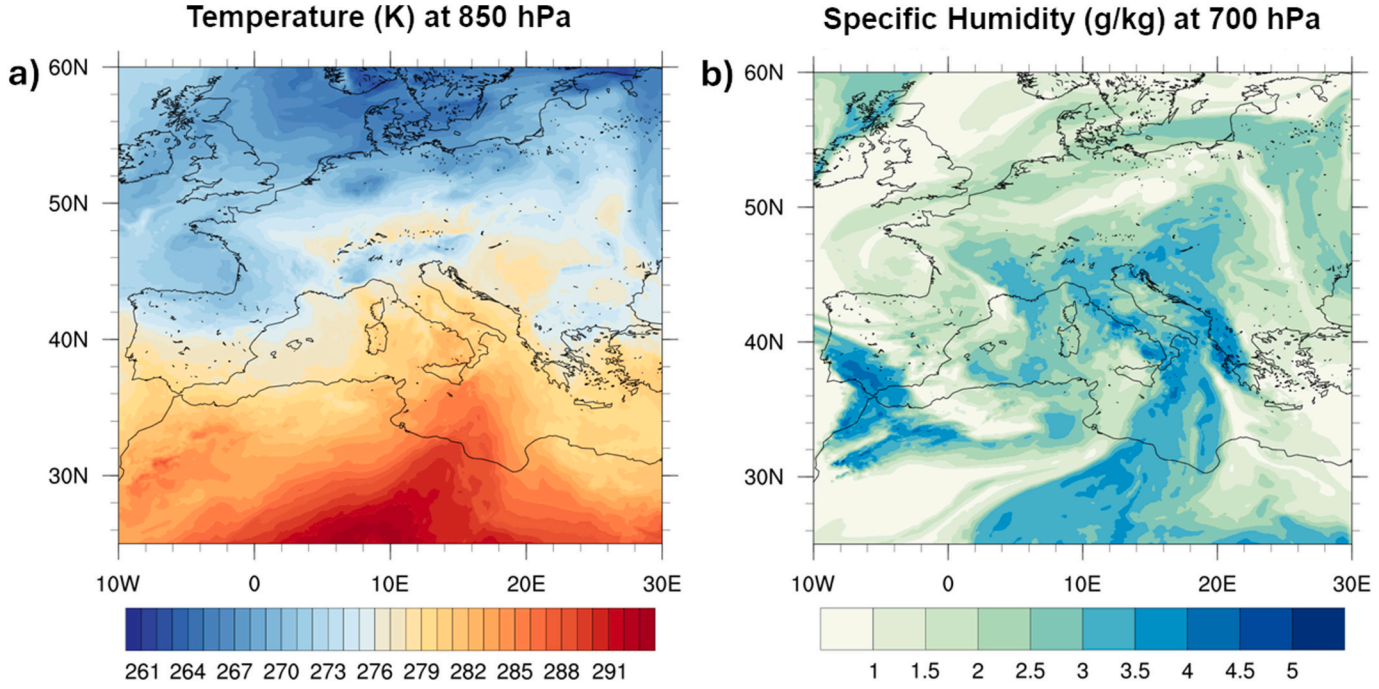


**Fig. 6.** (a) Temperature (K) at 850 hPa and (b) specific humidity (g/kg) at 700 hPa at 18 UTC, 03 December 2022.

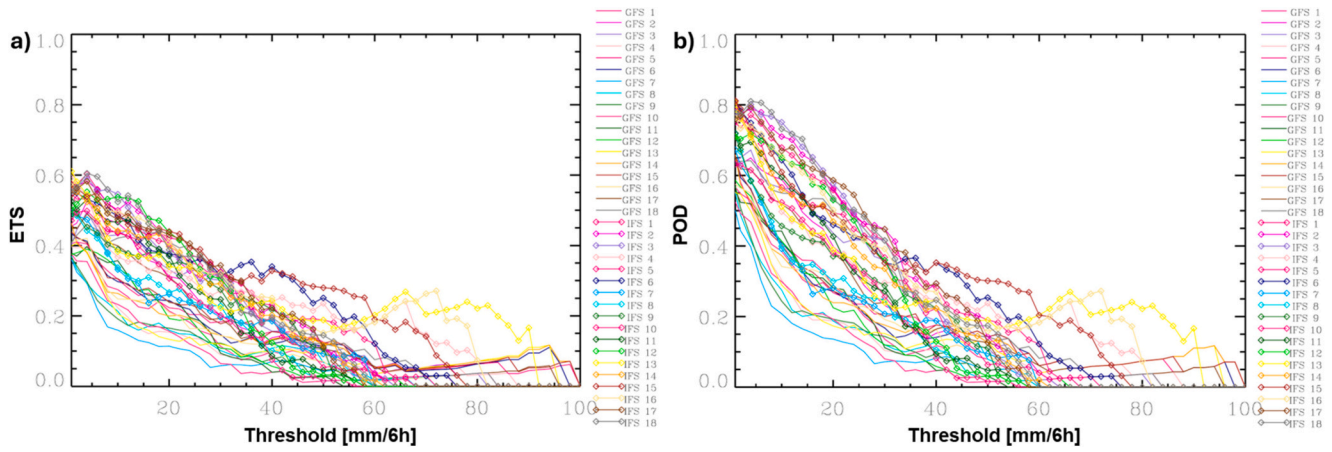


**Fig. 7.** (a) ETS and (b) POD scores of the different model configurations for the 6 h precipitation; the four 6 h phases, from 12 UTC on 3 December to 12 UTC on 4 December, are considered.

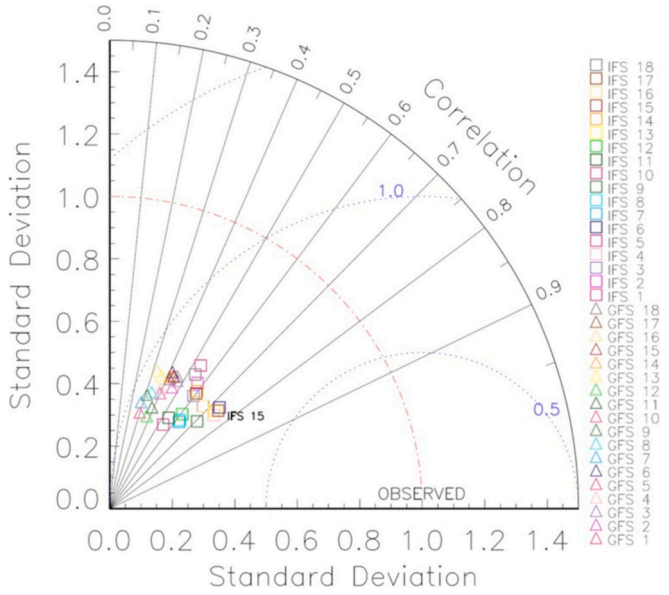


**Fig. 8.** Taylor diagram of the different model configurations for the 6 h precipitation; the four 6 h phases, from 12 UTC on 3 December to 12 UTC on 4 December, are considered.

of maximum reflectivity on the eastern side of the region, corresponding to the maximum accumulated rainfall in the region; the simulated system appears only slightly further south than the observed one. This comparison shows the ability of the model to correctly reproduce the main features of the weather pattern affecting southern Italy during the study period.

We also show the simulated 24 h accumulated rainfall map in Fig. 10a; this map is directly comparable with the observed rainfall maps (Fig. 3) reported at the beginning of Section 3. The rainfall pattern is well represented by the forecast; however, differences arise at the local scale. Specifically, the precipitation amount is generally underestimated over Sicily and Calabria, although the precipitation pattern is well reproduced. Especially in Sicily (first phase of the event) the highly localized precipitation peaks (values >200–250 mm / 24 h recorded in some stations; see Fig. 3) are not correctly simulated in quantitative terms, although the area affected by the rainfall has been identified by the model. Also, on the Calabrian Ionian side the CTL run simulates intense rainfall (locally greater than 80 mm / 24 h; sufficient for issuing civil protection alerts) but still lower than the rainfall recorded in specific areas (> 110 mm / 24 h in some stations; see Fig. 3). Finally, a generalized overestimation of rainfall in the Apulia region is also evident.

All in all, the results of this section show that, even if the forecast was able to predict the occurrence of a severe convective event over Sicily, Calabria and Apulia, the results are sensitive to both the physical parameterization used and to the IC/BC.

### 3.3.2. *Sensitivity tests*

Sensitivity analyses with the WRF model are commonly performed for the simulation of intense convective events. Most of these studies lead to the identification of optimal WRF configurations for the forecasts (e.g., Biswasharma et al., 2024; Solano-Farias et al., 2024), while other studies are more focused on evaluating the role of specific forcings, such as orography, heat fluxes or SST.

Below are some examples, certainly not exhaustive, of sensitivity analyses conducted with the WRF model for the study of convective events.

A recent study of Avolio and Federico (2018) can be considered as a reference for the results achieved in this work, mainly because it concerned the same area, studied an analogous event and adopted a similar methodology; in the "Summary and conclusions" section we will provide some comments aimed at comparing the two studies. In the aforementioned "Raganello flood" case (Avolio et al., 2019), the authors performed several preliminary tests, changing WRF schemes for microphysics / cumulus / radiation / boundary layer, to find a better-performing configuration for a highly localized convective event. Cassola et al. (2015) performed an intercomparison of eight different microphysics parameterization schemes available in WRF, for three different convective events affecting northern Italy, finding a set of best-performing configurations and assessing the important role of the horizontal resolution of the model. Regarding the role of the model grid spacing both Caccamo et al. (2017) and Castorina et al. (2022) assessed the impact of different grid resolutions of WRF for the forecasting of two flood events in southern Italy. A comprehensive analysis of a localized flash-flood event over the central Mediterranean was carried out by Gascón et al. (2016), through several experiments confirming the importance of the planetary boundary layer and microphysics parameterization schemes for a correct simulation of the event, as well as the need for high model horizontal resolution able to well represent the orography at small scales. Ferrari et al. (2023) recently performed a wide cascade sensitivity test with WRF for the simulation of deep convective events, changing cloud microphysics / planetary boundary layer / surface layer / and land-surface model parameterizations, for four significant precipitation events occurred in Northern Italy; the authors found a relevant role of PBL schemes and land-surface models, as

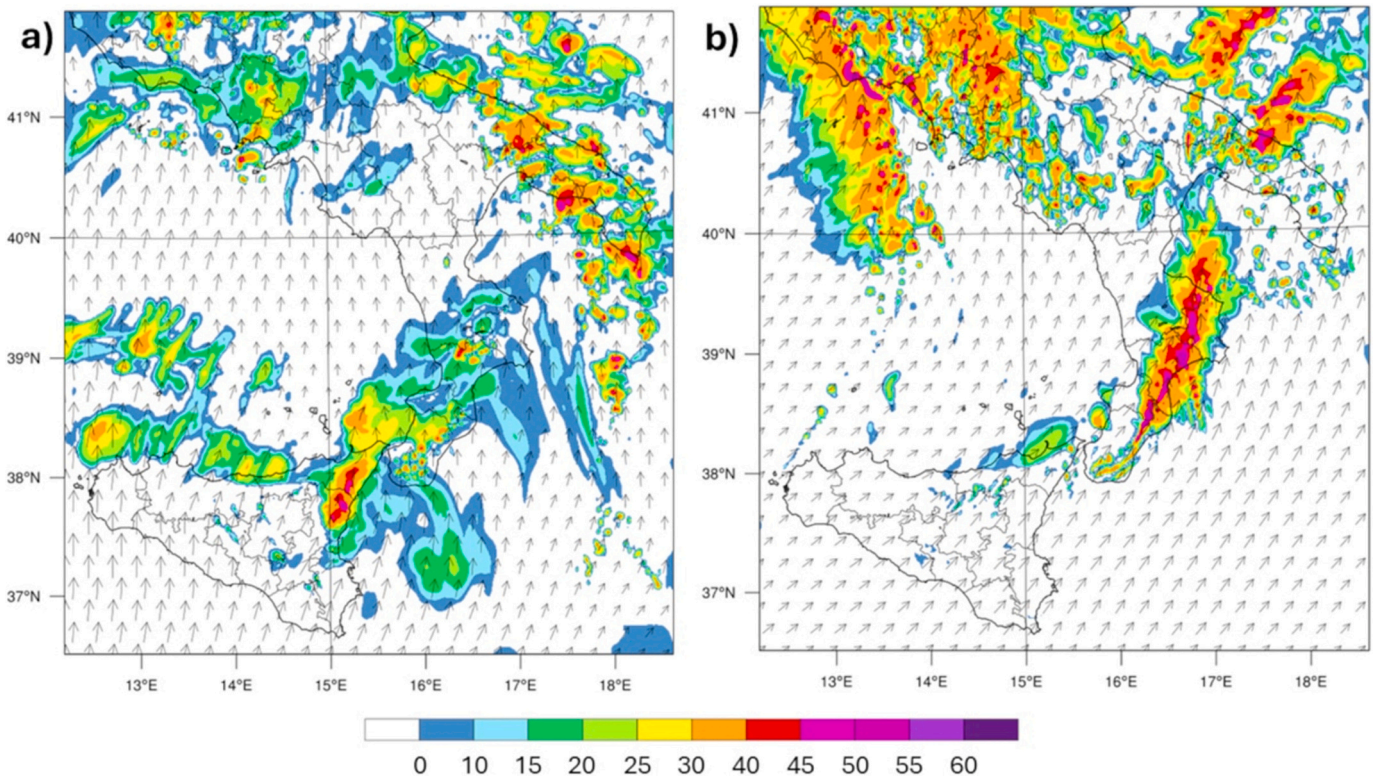


**Fig. 9.** Maximum reflectivity (dBZ) and wind vectors at 700 hPa simulated by the WRF model (2 km grid) at (a) 12 UTC, 03 December 2022 and (b) at 00 UTC, 04 December 2022.

well as of cloud-ice in the correct description of the events.

A number of studies have also addressed the role of the SST and topography in the convective events development. For example, Ricchi et al. (2023) studied a large-hail storm event on the Adriatic Sea, assessing the role of mountains (for the position of the storm cell) and of SST (for the storm development and the air-sea fluxes contribution). Marín et al. (2020) performed sensitivity tests to topography and SST on tornadoes in Chile, finding a significant role for such forcing factors in increasing atmospheric instability and in favoring tornadogenesis conditions in the area. Finally, also Avolio and Miglietta (2021) performed sensitivity experiments artificially varying the SST over a Mediterranean WRF domain, to estimate possible changes on instability parameters and tornadic supercells intensity.

In this section we address the discussion regarding the 3 additional sensitivity tests carried out to evaluate the role of convection parameterization ("CU" run), of a better prescription of SST ("SST" run) and of the horizontal resolution ("1 km" run). Also, in this case we computed both categorical scores and quantitative metrics considering short-term precipitation forecast (6 h), as well as producing the 24 h cumulative rainfall maps. These results are compared with the run previously identified as the best performing (CTL run). It is important to note that the quantitative metrics and the categorical scores discussed in this and in the next section have been computed for the domain of the 1 km grid, in order to compare the results of all configurations also with the 1 km run. The 1 km domain is smaller than that of the other simulations (as can be seen by comparing panels 10a, 10b and 10c with 10d). For this reason, the quantitative metrics and the categorical score of the same simulation (for example CTL) are slightly different in this and in the next section compared to Figs. 7 and 8.

Figure 10 shows the 24 h accumulated rainfall, i.e., from 12 UTC on 3 December to 12 UTC on 4 December, for the CTL run and for the three sensitivity tests. The qualitative scores for these sensitivity tests are shown in Fig. 12, which is further discussed in the next Section. In order to avoid the repetition of too similar maps we have added, in the same figure, also the scores of the 3DVAR experiment ("WRF_ASSIM" run hereafter) which will be discussed in the Section 3.2.3. Below, instead, we anticipate the results of the scores for the three sensitivity tests.

The CU run (Fig. 10b) simulates higher rainfall amounts in all three regions. A clear overestimation, mainly in terms of spatial extent of the rainfall pattern, is apparent in eastern Calabria and Apulia. This effect leads to an apparent improvement in performance in terms of scores (see orange curve in Fig. 12); this improvement, however, is counterbalanced by high FAR values (not shown) for all the considered thresholds. In particular, the FAR is almost 1 for precipitation larger than 60 mm / 6 h. Even if the POD and ETS have good performance, the usefulness of this configuration is limited by the high number of false alarms, and the results of this section show that (for this case study) the cumulus parameterization should not be used at convection permitting horizontal resolution.

The SST run (Fig. 10c) appears very similar to CTL, denoting a negligible role from the use of a higher spatial resolution analysis of the SST field. Considering the scores in Fig. 12 we see how the two runs are very similar for thresholds <40 mm / 6 h; for higher thresholds there is a general worsening of the performances. The 1 km run (Fig. 10d) appears to be the best sensitivity test, considering the daily rainfall map. In terms of scores, this run shows a general improvement of the performance for all thresholds, in particular for thresholds higher than 60 mm / 6 h (see the green curve in Fig. 12). Furthermore, the FAR values of the 1 km run are the lowest for all the considered thresholds. This result suggests that the use of a WRF domain with higher resolution compared to CTL leads to a clear improvement of the forecast by improving the POD and reducing the FAR (Lynn et al., 2020).

All in all the results of this section show that: a) the forecast of the event is not substantially influenced using a better prescription of SST; b) using the convection parameterization at the convection permitting horizontal resolution has a negative impact on the model forecast; c) using the 1 km horizontal resolution has a positive impact on the precipitation forecast, even if compared to an already good forecast of a

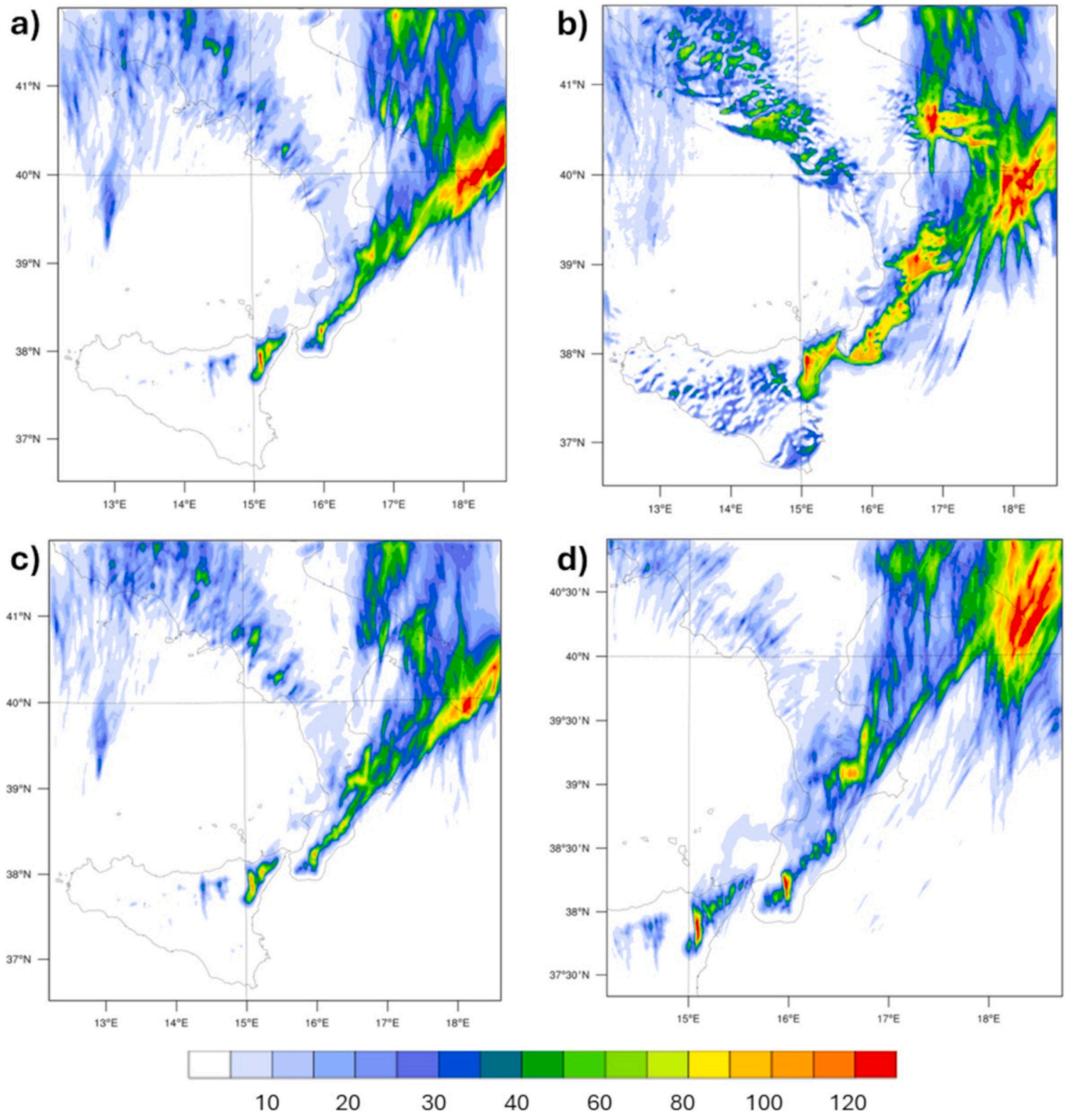


**Fig. 10.** WRF simulated rainfall (mm) between 12 UTC on 3 December 2022 and 12 UTC on 04 December 2022 for (a) the CTL run and for the tests: (b) CU, (c) SST and (d) 1 km.

convection permitting horizontal resolution (2 km).

The results of this Section will be further discussed at the end of the Section 3.3.3 where a (cumulative) Taylor diagram (Fig. 13) will be considered.

### 3.3.3. *Data assimilation experiment*

The above analysis shows that several WRF configurations, especially the CTL, well predicted the severity of this event. A possible way to refine the prediction as the storm is approaching or occurring, in order to take immediate actions to reduce its impact, is through data assimilation. Here we show the results of the data assimilation experiment, introduced in Section 2.2, assimilating lightning and CAPPI of radar reflectivity every 6 h and issuing the forecast for the next 6 h. An additional verification, at higher temporal resolution, is provided in Appendix A.

The rain forecast for the 6 h intervals from 12 to 18 UTC on 3 December to 06–12 UTC on 4 December are shown in the bottom panels of Fig. 11. In the same figure (upper panels) are also reported the 6 h forecast rain maps for the CTL run, in order to compare them with the WRF_ASSIM test.

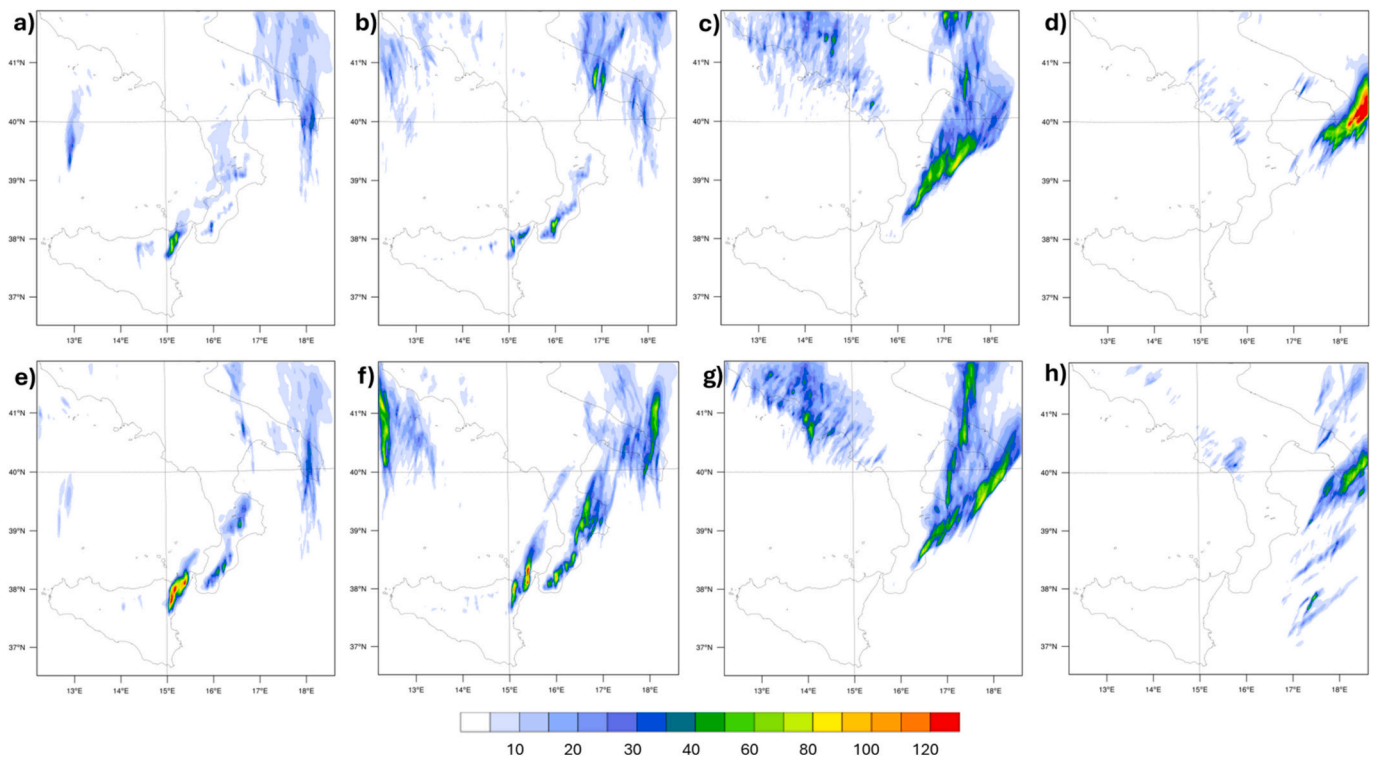


**Fig. 11.** 6 h WRF rainfall forecast (mm) for the CTL run (upper panels) and WRF_ASSIM experiment (lower panels), for the time intervals: (a,e) 12–18 UTC, 03 December 2022; (b,f) 18–24 UTC, 03 December 2022; (c,g) 00–06 UTC, 04 December 2022 and (d,h) 06–12 UTC, 04 December 2022.

There are few points to notice: in the first phase (between 12 and 18 UTC on 3 December), when heavy precipitation impacted Sicily, the WRF_ASSIM experiment is better able to predict the heavy precipitation amount over the Northeastern part of the Region with values larger than 120 mm / 6 h; of course, the CTL run still suggest a high impact weather event occurring there, nevertheless the severity of the event is better represented in the WRF_ASSIM experiment. The phase 18–24 UTC also shows a significant impact of data assimilation in predicting the severity of the storm. Abundant rainfall is predicted over Eastern Calabria with observations larger than 50 mm / 6 h in several places. Most of this precipitation is missed by the CTL run, while it is well represented in WRF_ASSIM. During the following phase, 00–06 UTC, heavy precipitation (and a tornado; see Section 3.3) occurred over the Central-Eastern Calabria. This rainfall is well represented by the CTL run, while it is slightly underestimated by WRF_ASSIM. This decrease is determined by the fact that the storm moves faster towards East when data assimilation is applied, and this determines a lower amount of precipitation accumulated over Eastern Calabria. The faster movement of the storm towards East when data assimilation is applied is confirmed by the larger precipitation accumulated in the WRF_ASSIM experiment over Apulia. The comparisons of rainfall forecast by WRF_ASSIM, CTL run and observations for this phase, show that CTL run has a better agreement with observations; in addition, using 3DVAR has also a negative impact on the tornado forecast that occurred in this phase (See section 3.3). For the last phase, 06–12 UTC on 4 December, the impact of 3DVAR is mainly a reduction of the rainfall prediction over Apulia. The comparison with

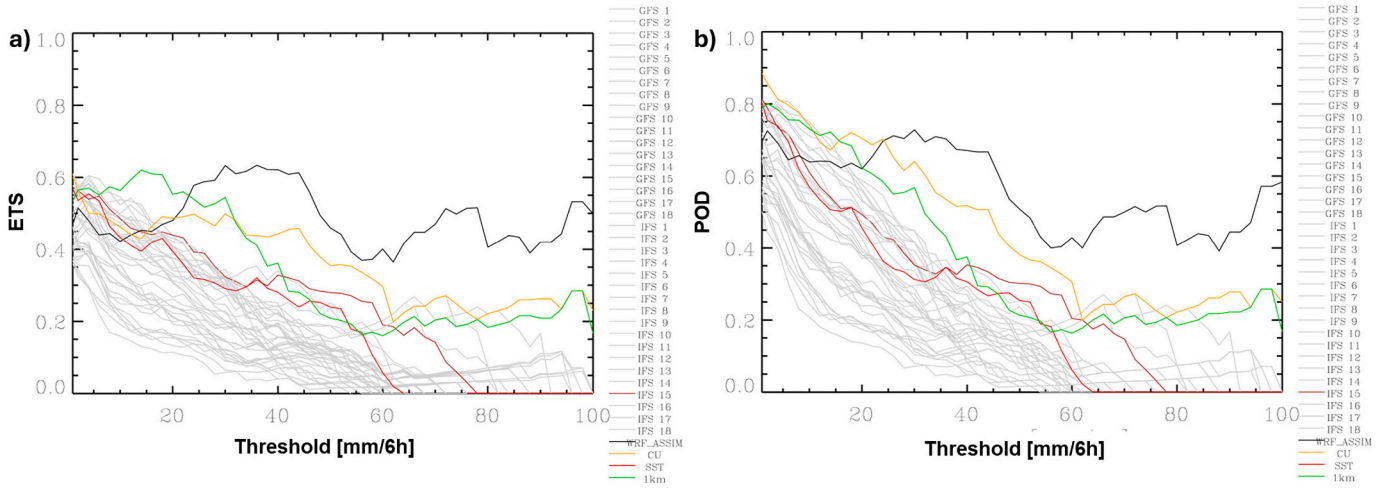


**Fig. 12.** (a) ETS and (b) POD scores of the different model configurations for the 6 h precipitation. Gray curves represent all the initial runs (already shown in Fig. 7); the CTL run is in dark red, the WRF_ASSIM experiment is in black, the SST is in light red, the 1 km run is in green and the CU run is in orange. (For interpretation of the references to colour in this figure legend, the reader is referred to the web version of this article.)

observations shows that the CTL run overestimated the rainfall over Southern Apulia and WRF_ASSIM has a better agreement with observations.

All in all, the 3DVAR clearly improves three out of the four phases considered for this event. This is confirmed by the analysis of the ETS and POD scores (Fig. 12) for the four phases. It is apparent that, except for thresholds below 20 mm/3 h, where some other configuration - including the CTL run - have better performance, WRF_ASSIM is the only experiment having a POD larger than 50 % for all thresholds up to 100 mm / 6 h. The good performance of the WRF_ASSIM experiment is confirmed by the analysis of the Taylor diagram (Fig. 13). The WRF_ASSIM forecast improves the correlation and the representation of the observed precipitation standard deviation. We also note that the performance of SST is slightly lower than CTL, while the 1 km has a better performance than CTL because it represents more consistently the observed rainfall standard deviation. Also, the CU forecast has a better representation of the observation standard deviation, nevertheless the high number of false alarms prevents a useful adoption of the CU forecast. This is indirectly confirmed by the lower correlation of the precipitation forecast of CU compared to CTL, WRF_ASSIM and 1 km.

The results of this section clearly show that the data assimilation is very useful in the prediction of severe weather events and can be used to refine, even if not for all the phases of the storm evolution, the performance of the model forecast. However, as discussed also in the next section, WRF_ASSIM is not always the best forecast and there are possible paths of improvement. First, the assimilation of additional data as surface stations, GNSS-ZTD or radiosoundings is useful to refine the forecast as they can help to better represent the vertical structure of the atmosphere, as well as converging areas that could give a better positioning of convective cells at the assimilation time and of their evolution at the short-range. Second, the horizontal resolution of the WRF_ASSIM experiment can be enhanced to simulate in more detail the interaction between the local orography and the atmosphere, and this aspect is of importance especially in complex orography as in the regions hit by this storm. This is also shown by the good performance of the 1 km sensitivity test compared to the CTL run. Third, there is space for improvement of the 3DVAR settings as in this work radar observations are superobbed at 5 km horizontal resolution and the correlation of the observations error is neglected. While we cannot provide simulations considering this point, as radar observations are saved at 5 km horizontal resolution, considering the observation error correlation in the 3DVAR scheme can improve the performance of the forecast with data assimilation because more observations are assimilated at higher horizontal resolution. A method to define the error decorrelation length-scale is that discussed in Desroziers et al. (2005), that could be applied in future studies to assimilate observations at higher horizontal resolution.

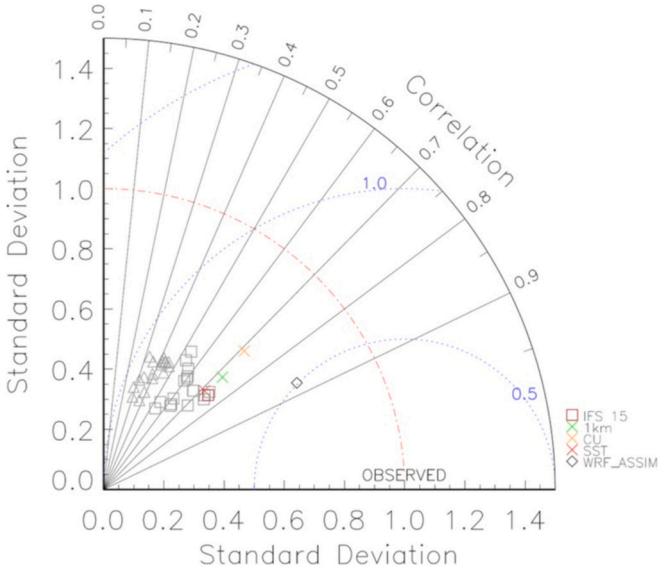


**Fig. 13.** Taylor diagram of the different model configurations for the 6 h precipitation; the four 6 h phases, from 12 UTC on 3 December to 12 UTC on 4 December, are considered. CTL, WRF_ASSIM, CU, 1 km and SST are highlighted.

This section concludes the analysis of the precipitation forecast for time intervals of 6 h. As the event was rapidly evolving it is also interesting to evaluate the precipitation forecast for shorter time scales. Appendix A shows the POD and ETS scores and the FSS for time intervals of 3 h. Compared to the results presented in this Section (Fig. 12) the verification for 3 h time intervals shows lower performance. This is expected as we are requesting a larger precision in the timing of the prediction. In addition, the relative performance of the different WRF configurations is similar to that presented in this Section 3.2, with WRF_ASSIM performing the best followed by 1 km, CTL and SST. The CU forecast has a large POD, but also a larger FAR compared to CTL, limiting the practical application of this forecast.

### 3.4. Tornado forecast

An EF2 tornado affected Isola di Capo Rizzuto (Northeastern Calabria; see purple circle in Fig. 1c) at 03 UTC on 04 December 2022. According to PRETEMP, several damages to buildings and cars were reported; moreover, several trees were uprooted or snapped, and three camping sites were severely damaged.

A goal of this study is to test the forecasting capabilities of WRF also in predicting the tornado affecting Calabria, both considering the previously recognized best run (CTL) and also assessing the possible improvement of using other modeling configurations.

A recent updated climatology of tornadoes in Italy (Avolio and Miglietta, 2021, 2023) confirmed that the southeastern regions of the Italian peninsula, eastern Calabria and Apulia in particular, are among the areas most affected by tornadoes in the Mediterranean. Several works studied some cases of tornado in southern Italy (Miglietta and Rotunno, 2016; Miglietta et al., 2017a, 2017b; Avolio and Miglietta, 2021, 2022) throughout numerical simulations, mainly aimed at reproducing the structure and the track of the convective cells responsible for tornadoes, as well as at simulating the environmental conditions more favorable for tornado formation, considering specific instability parameters/indices and comparing them with their critical thresholds (assessed by literature). The approach of identifying an environment potentially favorable to the occurrence of tornadoes or severe thunderstorms was adopted in several studies (in addition to the works just mentioned for southern Italy), both in the USA (e.g., Rasmussen and Blanchard, 1998; Craven and Brooks, 2004; Brooks, 2013) and in Europe (e.g.; Groenemeijer and van Delden, 2007; Grunwald and Brooks, 2011; Taszarek et al., 2017; Rodriguez and Bech, 2018). Many of these have used observations (proximity soundings), while other studies have successfully adopted modeling outputs (reanalysis).

Here we consider some of the atmospheric parameters / instability indices, widely used to predict the environmental conditions potentially favorable for the occurrence of tornadoes. A key role is played by the Convective Available Potential Energy (CAPE) and the wind shear in different layers, i.e., Deep Layer Shear (DLS; 0–6 km) and Mid-Level Shear (MLS, 0–3 km). Values of CAPE >2000–2500 $JKg^{-1}$ are associated with supercell potential / strong instability, often conductive of tornadoes, as well as values of DLS (MSL) > 25–30 (15–20) $ms^{-1}$. Another important diagnostic field is the updraft helicity (UH) (Kain et al., 2008) that identifies the strength of rotating updrafts in storms. The efficacy of UH in forecasting mid-level mesocyclones is widely recognized, and the use of UH as a possible tornado proxy was documented in several papers, especially in the US (e.g., Clark et al., 2012), often combined with other environmental parameters and diagnostics (Rasmussen and Blanchard, 1998; Thompson et al., 2004; Grunwald and Brooks, 2011; Grams et al., 2012; Gallo et al., 2016). A typical assumed

threshold to forecast such events is UH = 50 $m^2s^{-2}$ (Clark et al., 2012). Although not sufficient (if used alone) for determining tornado probability, this field can be useful to identify the possible cell (supercell / mesocyclone) from which the tornado originated, once the occurrence of the tornado has been confirmed by observations (as in our case).We base our analysis on the CTL run. In the hours preceding the development of the tornado high values of most unstable CAPE (> 2000 J/kg) over Ionian and Tyrrhenian Seas, as well as moderate-to-high vertical MSL (locally >20 m/s), were simulated (not shown). In both cases these values exceed the thresholds defined above and show an environment prone to instability conditions.

In Fig. 14 we report the observed composite radar reflectivity (left panel) and the maximum reflectivity (right panel) simulated by WRF at 03 UTC on 4 December, i.e., at the time corresponding to the tornado report. The maximum reflectivity simulated by WRF is consistent with the observed pattern, showing a good agreement between them. We can see, in particular, the narrow area on the eastern side of the Calabria region, just corresponding to the tornado location, with values exceeding 45 dBz.

To further assess the skill of the model in simulating the convective cells responsible for the tornadoes we also report in Fig. 15 (upper panels) the UH simulated by WRF at 03 UTC on 04 December (left panel refers to CTL). The map shows several localized areas with values of UH greater than 100 $m^2/s^2$, indicating strong helicoidal ascending motion typical of a well-developed convective cells / supercell. The location of the larger UH relative maximum area over Isola capo Rizzuto, indicates a very good simulation performed by WRF for this event.

Since the WRF_ASSIM run was found to be better-performing for the short-term precipitation forecast (see Section 3.2.3), we compared its prediction of UH (Fig. 15b) with the CTL run (Fig. 15a). From Fig. 15b it is apparent that the UH simulated by the WRF_ASSIM run is worse compared to CTL. In this case, in fact, an evident "timing" error is attributable to WRF_ASSIM that simulates convective cells displaced in the open (Ionian) sea, at the time of the tornado report (03 UTC). As shown in Section 3.2.3, the storm simulated by WRF_ASSIM moves faster than other simulations eastwards, and the exact timing of the tornado occurrence is missed by WRF_ASSIM.

To better interpret this displacement, mainly attributable to the different model forecast of wind fields, we report in the bottom panel of Fig. 15 the wind at 700 hPa (a level often taken into account to identify possible tornado spawning cells; i.e. Avolio and Miglietta (2022)) simulated both by CTL run (left) and WRF_ASSIM run (right). The WRF_ASSIM run simulates a wind more intense than CTL over a large part of the Ionian Sea, between Calabria and Apulia, with wind differences that locally exceed 10 m/s.

The results of this section show that even if data assimilation can improve the short-term precipitation forecast for the case study, it doesn't improve all the aspects of the forecast, such as the simulation of the wind fields and the tornado, for which the CTL run has a better performance. Paths for improving the WRF_ASSIM forecast have been highlighted in the previous section and need to be explored in future works, nevertheless, it is also important to note that the WRF_ASSIM forecast predicted conditions favorable to supercell formation with possible tornado occurring one hour before the real occurrence of the event. The good performance of CTL and, to a lesser extent, of WRF_ASSIM, suggests that this tornado case was especially predictable (a condition not always satisfied for such particular events).

## 4. Summary and conclusions

This paper shows the verification and sensitivity tests for a multi-hazard event occurred in Southern Italy between 03 and 04 December 2022. The severity of the event was determined by favorable large scale synoptic conditions and by the interaction of the synoptic scale flow with the local orography. Large scale flow was directed from S-SW towards southern Italy bringing moist and unstable air masses. The orographic uplift triggered vigorous convection, heavy rainfall was recorded in three regions (Sicily, Calabria and Apulia) and a tornado was reported in central-eastern Calabria.

This event was simulated by WRF using different settings of the planetary boundary layer, cumulus and microphysics parameterization schemes (18 configurations) and for two different sets of initial and boundary conditions (ECMWF-IFS and NCEP-GFS).

Results show, in general, a good prediction of the precipitation event, as most of the configurations are able to simulate the heavy rainfall that characterized this event. However, when ECMWF-IFS IC/BC are used,

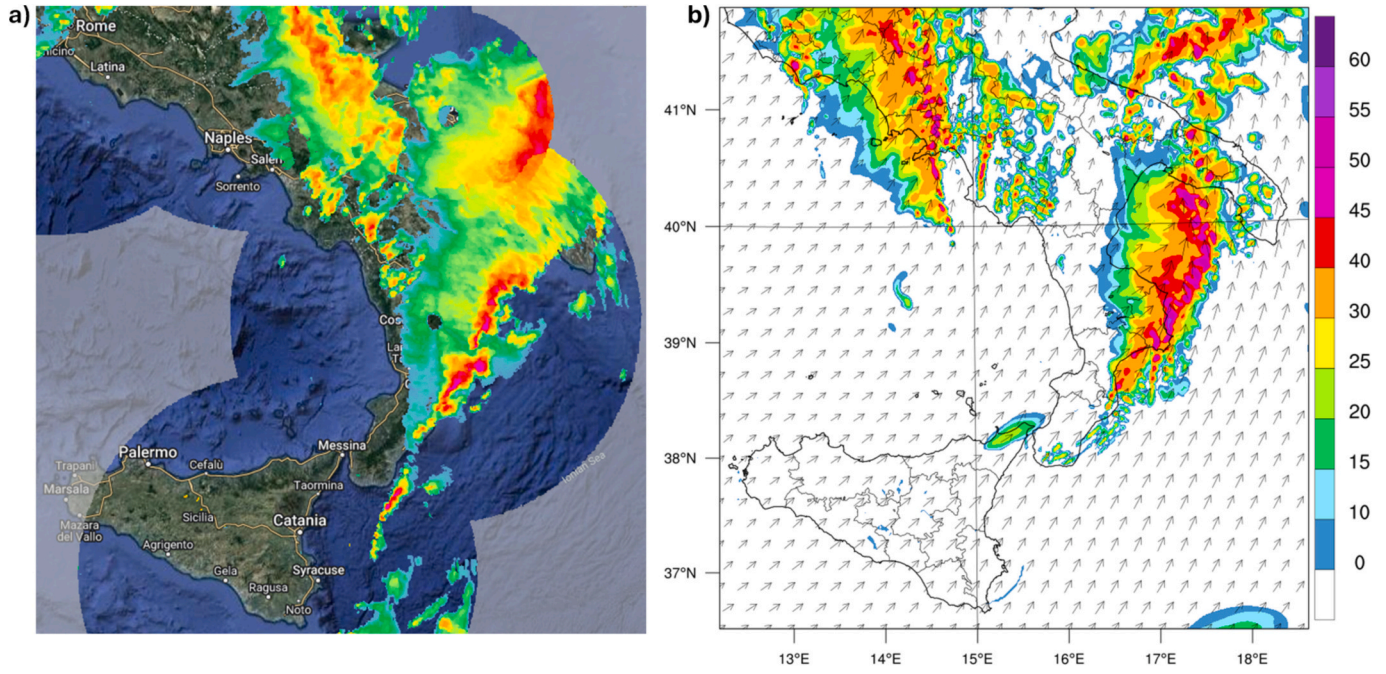


**Fig. 14.** (a) Composite radar reflectivity (dBZ) and (b) maximum reflectivity (dBZ) and wind vectors at 700 hPa simulated by the WRF model (CTL); both maps refer to 03 UTC, 04 December 2022.

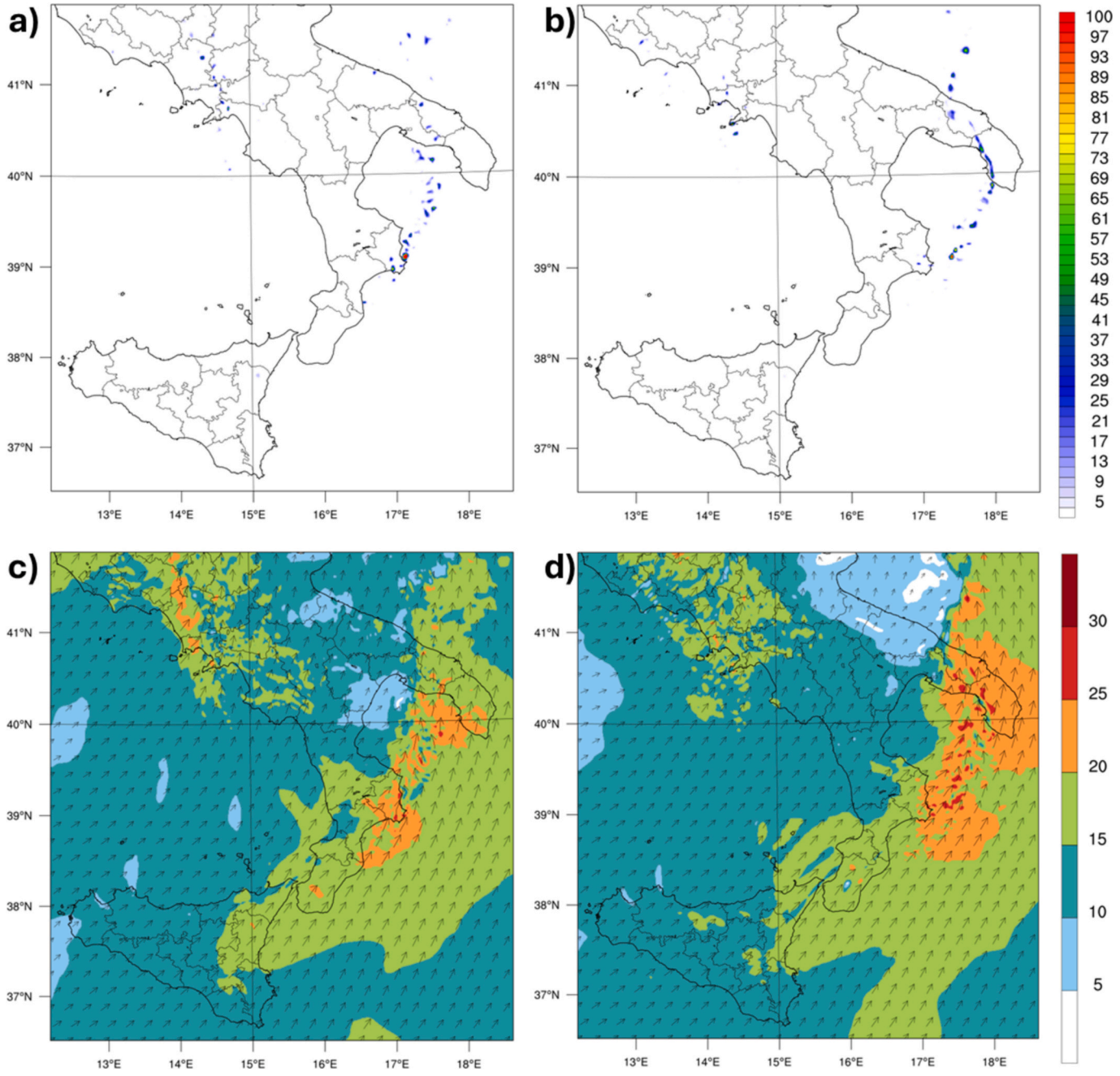


**Fig. 15.** Updraft Helicity (m2/s2) simulated by WRF for (a) CTL and (b) WRF_ASSIM; wind vectors and wind speed (m/s) at 700 hPa for (c) CTL and (d) 3DVAR. All maps refer to 03 UTC, 04 December 2022.

WRF has a better forecast at the local scale, enhancing both its spatial representation and the amount of precipitation, as shown by the better values of the statistical scores. As expected, IC/BC have an important impact on the forecast of severe weather events, and this is confirmed by the results of this paper.

While most of the simulations are able to forecast the occurrence of a severe convective event for the three regions Sicily, Calabria and Apulia, there are substantial differences at the local scale. In particular, the simulation with WSM7 for microphysics, KF for the cumulus convection parameterization over the mother domain and YSU for PBL performs better than other configurations as it better represents the spatio-temporal evolution of the storm and the precipitation amounts. Further sensitivity tests were performed using a more detailed input for SST, the activation of the cumulus parameterization for the 2 km horizontal resolution domain and using a higher horizontal resolution for the inner domain (1 km); these simulations were compared with the CTL run. Results show that using the cumulus convection parameterization for the inner domain has a negative impact on the forecast, as it causes many false alarms over the three regions; using the improved SST has a negligible impact for this event; refining the resolution improves the quality of the forecast as the intensity of the precipitation is better determined, especially over Sicily and Calabria, and false alarms are reduced.

Finally, the best forecast (CTL) is compared with a simulation using lightning and radar reflectivity data assimilation (WRF_ASSIM). The latter provides the forecast at the short range in a RUC of 6 h. The results reveal that the precipitation forecast of WRF_ASSIM is better than CTL for all forecast phases. This result shows again that RUC simulations

with data assimilation are able to refine the forecast at the local scale for deep convective events as the storm is approaching (Federico et al., 2024). However, not all the aspects of the forecast are improved by data assimilation and, in particular, the forecast of the tornado that occurred over Calabria is better forecast by CTL than by WRF_ASSIM. Specifically, WRF_ASSIM causes the storm to move faster towards East compared to observations and the forecast of the tornado is anticipated by 1 h with respect to the real occurrence, while CTL does a very precise forecast in time and space. Possible ways to improve the data assimilation forecast have been outlined.

In a previous paper, Avolio and Federico (2018) adopted a similar approach for the forecast of a severe convective storm over Calabria. The results of this paper extend their finding in two main directions: first it is shown that enhancing the horizontal resolution can be useful for improving the forecast at the local scale, second it is shown that RUC cycle with data assimilation can be useful to refine the forecast when the storm is approaching or occurring. For the first point, in particular, Avolio and Federico (2018) considered the 1 km horizontal resolution over Calabria, nevertheless their analysis considered rainfall thresholds much lower than those of this paper and they concluded that the 1 km horizontal resolution had a positive but small impact on the precipitation forecast. In this paper, we extend this result showing that the higher horizontal resolution can improve the quality of the forecast, especially when high precipitation is considered (in this paper rainfall larger than 40 mm / 6 h). Finally, the focus on the tornado extends the analysis done in the previous paper. Of course, the usefulness of using many simulations with different WRF configurations, as those shown in this paper or in Avolio and Federico (2018), is determined by the fact that many configurations correctly forecasted the severity of the event, showing a high probability of occurrence of a severe storm.

It is important to highlight that the results of this paper refer to a case study only and it will be important to test, in future works, the proposed methodology for multiple similar cases, in order to improve the robustness of the results. However, what is exportable is the methodology proposed and some specific results. The methodology is composed of two steps: first, running an ensemble of WRF simulations with members using different initial and boundary conditions and with different physical settings. The output of the ensemble provides information about the severity of the storm and its probability of occurrence. Then, a RUC forecast with data assimilation of observations at the local scale is used to refine the forecast while the event is occurring or approaching for fast response actions. About the specific results, the 1 km horizontal resolution experiment shows that the horizontal resolution of the ensemble and of the RUC cycle should be high to better represent the interaction between the storm and local orography.

Despite the potential of the approach proposed in this paper for the prediction of severe weather events, there are some limitations in this study. Limits in the 3DVAR have been already discussed in Section 3.2.3. However, there are limitations in the WRF setting itself. First, the ensemble doesn't account for some important physical parameterizations as, for example, double moment microphysics schemes. Second, we used the different runs of WRF to show the high probability of occurrence of a severe weather event as many members predicted heavy rainfall in southern Italy. A better forecast could be attained optimally combining the output of the different WRF configurations (multi-physics ensemble) with observations, hopefully improving the forecast for time ranges longer than 6 h. Nevertheless, a large number of cases should be considered for the setting of the multi-physics ensemble. Finally, in a recent study, Lagasio et al. (2022) combined the output of different WRF runs with observational nowcasting to improve the forecast of convective events. The combination gives more weight to the forecasts that were more in agreement with rainfall observations at the run-time, resulting in an improvement of the performance compared to the initial unweighted forecasts. This research will be the focus of future studies.

## CRediT authorship contribution statement

**E. Avolio:** Writing – review & editing, Writing – original draft, Validation, Software, Methodology, Investigation, Formal analysis, Conceptualization. **G. Castorina:** Writing – review & editing, Validation, Software, Data curation. **R.C. Torcasio:** Writing – review & editing, Validation, Software, Investigation. **S. Federico:** Writing – review & editing, Writing – original draft, Validation, Investigation, Formal analysis.

## Declaration of competing interest

The authors declare that they have no known competing financial interests or personal relationships that could have appeared to influence the work reported in this paper.

## Data availability

Data will be made available on request.

## Acknowledgments

This work was funded by the Next Generation EU - Italian NRRP, Mission 4, Component 2, Investment 1.5, call for the creation and strengthening of 'Innovation Ecosystems', building 'Territorial R&D Leaders' (Directorial Decree n. 2021/3277) - project Tech4You - Technologies for climate change adaptation and quality of life improvement, n. ECS0000009. This work reflects only the authors' views and opinions, neither the Ministry for University and Research nor the European Commission can be considered responsible for them.

The Italian Department of Civil Protection is acknowledged for the radar images (derived by the automatic system Dewetra), for the radar data and for the raingauges data. LINET data were granted through the agreement for cooperation between CNR- ISAC and Nowcast GmbH (https://www.nowcast.de/en). ECMWF is acknowledged for providing part of the computational time required for this work through the special project SPITFEDE.

## Appendix A. Supplementary data

Supplementary data to this article can be found online at https://doi.org/10.1016/j.atmosres.2024.107827.

## References

Aronica, G.T., Brigandí, G., Morey, N., 2012. Flash floods and debris flow in the city area of Messina, north-east part of Sicily, Italy in October 2009: the case of the Giampilieri catchment. Nat. Hazards Earth Syst. Sci. 12 (5), 1295–1309. https://doi.org/10.5194/nhess-12-1295-2012.

Avolio, E., Federico, S., 2018. WRF simulations for a heavy rainfall event in southern Italy: verification and sensitivity tests. Atmos. Res. 209, 14–35. https://doi.org/10.1016/j.atmosres.2018.03.009.

Avolio, E., Miglietta, M.M., 2021. Multiple tornadoes in the Italian Ionian regions: observations, sensitivity tests and mesoscale analysis of convective storm environmental parameters. Atmos. Res. 263, 105800. https://doi.org/10.1016/j.atmosres.2021.105800.

Avolio, E., Miglietta, M.M., 2022. Tornadoes in the Tyrrhenian regions of the Italian peninsula: the case study of 28 July 2019. Atmos. Res. 278, 106285. https://doi.org/10.1016/j.atmosres.2022.106285.

Avolio, E., Miglietta, M.M., 2023. A comparative analysis of two Mediterranean Tornado Hotspots. Atmosphere 14 (1), 189. https://doi.org/10.3390/atmos14010189.

Avolio, E., Cavalcanti, O., Furnari, L., Senatore, A., Mendicino, G., 2019. Brief communication: preliminary hydro-meteorological analysis of the flash flood of 20 August 2018 in Raganello Gorge, southern Italy. Nat. Hazards Earth Syst. Sci. 19 (8), 1619–1627. https://doi.org/10.5194/nhess-19-1619-2019.

Bae, S.Y., Hong, S.-Y., Tao, W.-K., 2019. Development of a single-moment cloud microphysics scheme with prognostic hail for the weather research and forecasting (WRF) model. Asia-Pac. J. Atmos. Sci. 55 (2), 233–245. https://doi.org/10.1007/s13143-018-0066-3.

Benjamin, S.G., Dévényi, D., Weygandt, S.S., Brundage, K.J., Brown, J.M., Grell, G.A., Kim, D., Schwartz, B.E., Smirnova, T.G., Smith, T.L., Manikin, G.S., 2004. An hourly

assimilation–forecast cycle: the RUC. Mon. Weather Rev. 132 (2), 495–518. https://doi.org/10.1175/1520-0493(2004)132<0495:AHACTR>2.0.CO;2.
Betts, A.K., Miller, M.J., 1986. A new convective adjustment scheme. Part II: single column tests using GATE wave, BOMEX, ATEX and arctic air-mass data sets. Quart. J. Royal Meteorol. Soc. 112 (473), 693–709. https://doi.org/10.1002/qj.49711247308.
Betz, H.D., Schmidt, K., Laroche, P., Blanchet, P., Oettinger, W.P., Defer, E., Dziewit, Z., Konarski, J., 2009. LINET—An international lightning detection network in Europe. Atmos. Res. 91 (2–4), 564–573. https://doi.org/10.1016/j.atmosres.2008.06.012.
Biswasharma, R., Umakanth, N., Pongener, I., Longkumer, I., Madan Mohan Rao, K., Pawar, Sunil D., Gopalkrishnan, V., Sharma, S., 2024. Sensitivity analysis of cumulus and microphysics schemes in the WRF model in simulating Extreme Rainfall events over the hilly terrain of Nagaland. Atmos. Res. 304. https://doi.org/10.1016/j.atmosres.2024.107393.
Brooks, H.E., 2013. Severe thunderstorms and climate change. Atmos. Res. 123, 129–138. https://doi.org/10.1016/j.atmosres.2012.04.002.
Brunner, J.C., Ackerman, S.A., Bachmeier, A.S., Rabin, R.M., 2007. A quantitative analysis of the enhanced-V feature in relation to severe weather. Weather Forecast. 22 (4), 853–872. https://doi.org/10.1175/WAF1022.1.
Caccamo, M.T., Castorina, G., Colombo, F., Insinga, V., Maiorana, E., Magazù, S., 2017. Weather forecast performances for complex orographic areas: Impact of different grid resolutions and of geographic data on heavy rainfall event simulations in Sicily. Atmos. Res. 198, 22–33. https://doi.org/10.1016/j.atmosres.2017.07.028.
Calvin, K., Dasgupta, D., Krinner, G., Mukherji, A., Thorne, P. W., Trisos, C., Romero, J., Aldunce, P., Barrett, K., Blanco, G., Cheung, W. W. L., Connors, S., Denton, F., Diongue-Niang, A., Dodman, D., Garschagen, M., Geden, O., Hayward, B., Jones, C., … Ha, M., 2023. IPCC, 2023: Climate Change 2023: Synthesis Report. Contribution of Working Groups I, II and III to the Sixth Assessment Report of the Intergovernmental Panel on Climate Change [Core Writing Team, H. Lee and J. Romero (eds.)]. IPCC, Geneva, Switzerland. Doi: 10.59327/IPCC/AR6-9789291691647.
Cassola, F., Ferrari, F., Mazzino, A., 2015. Numerical simulations of Mediterranean heavy precipitation events with the WRF model: a verification exercise using different approaches. Atmos. Res. 164–165, 210–225. https://doi.org/10.1016/j.atmosres.2015.05.010.
Castorina, G., Caccamo, M.T., Insinga, V., Magazù, S., Munaò, G., Ortega, C., Semprebello, A., Rizza, U., 2022. Impact of the Different Grid Resolutions of the WRF Model for the forecasting of the Flood event of 15 July 2020 in Palermo (Italy). Atmosphere 13 (10), 1717. https://doi.org/10.3390/atmos13101717.
Castorina, G., Semprebello, A., Insinga, V., Italiano, F., Caccamo, M.T., Magazù, S., Morichetti, M., Rizza, U., 2023. Performance of the WRF Model for the forecasting of the V-Shaped storm Recorded on 11–12 November 2019 in the Eastern Sicily. Atmosphere 14 (2), 390. https://doi.org/10.3390/atmos14020390.
Clark, A.J., Kain, J.S., Marsh, P.T., Correia, J., Xue, M., Kong, F., 2012. Forecasting Tornado pathlengths using a three-dimensional object identification algorithm applied to convection-allowing forecasts. Weather Forecast. 27 (5), 1090–1113. https://doi.org/10.1175/WAF-D-11-00147.1.
Craven, J.P., Brooks, H.E., 2004. Baseline climatology of sounding derived parameters associated with deep moist convection. Natl. Wea. Dig. 28, 13–24. Available online at: http://www.nssl.noaa.gov/users/brooks/public_html/papers/cravenbrooksnwa.pdf (last access 25 November 2024).
Davolio, S., Silvestro, F., Gastaldo, T., 2017. Impact of rainfall assimilation on high-resolution hydrometeorological forecasts over Liguria, Italy. J. Hydrometeorol. 18 (10), 2659–2680. https://doi.org/10.1175/JHM-D-17-0073.1.
De Martin, F., Carlon, N., Pavan, F., Carpentari, S., Giazzi, M., Peressutti, G., Miglietta, M.M., Davolio, S., 2023. Toward a Dedicated Warning System of Severe Storms in Italy: The PRETEMP Project, 11th European Conference on Severe Storms, Bucharest, Romania, 8–12 May 2023, ECSS2023–18. https://doi.org/10.5194/ecss2023-18.
Desroziers, G., Berre, L., Chapnik, B., Poli, P., 2005. Diagnosis of observation, background, and analysis error statistics in observation space. Q. J. Roy Meteor. Soc. 131, 3385–3396 doi: 10.1256/qj.05.108.
Doswell, C.A., Brooks, H.E., Dotzek, N., 2009. On the implementation of the enhanced Fujita scale in the USA. Atmos. Res. 93 (1–3), 554–563. https://doi.org/10.1016/j.atmosres.2008.11.003.
Dudhia, J., Hong, S.-Y., Lim, K.-S., 2008. A new method for representing mixed-phase particle fall speeds in bulk microphysics parameterizations. J. Meteorol. Soc. Japan Ser. II 86A, 33–44. https://doi.org/10.2151/jmsj.86A.33.
Faccani, C., Ferretti, R., Pacione, R., Paolucci, T., Vespe, F., Cucurull, L., 2005. Impact of a high density GPS network on the operational forecast. Adv. Geosci. 2, 73–79. https://doi.org/10.5194/adgeo-2-73-2005.
Federico, S., 2013. Implementation of a 3D-Var system for atmospheric profiling data assimilation into the RAMS model: initial results. Atmos. Meas. Tech. 6 (12), 3563–3576. https://doi.org/10.5194/amt-6-3563-2013.
Federico, S., Bellecci, C., Colacino, M., 2003a. Numerical simulation of Crotone flood: storm evolution. Il Nuovo Cimento C 26C, 357–371.
Federico, S., Bellecci, C., Colacino, M., 2003b. Quantitative precipitation of the Soverato flood: the role of orography and surface fluxes. Il Nuovo Cimento C 26 C, 7–22.
Federico, S., Petracca, M., Panegrossi, G., Dietrich, S., 2017. Improvement of RAMS precipitation forecast at the short-range through lightning data assimilation. Nat. Hazards Earth Syst. Sci. 17 (1), 61–76. https://doi.org/10.5194/nhess-17-61-2017.
Federico, S., Torcasio, R.C., Avolio, E., Caumont, O., Montopoli, M., Baldini, L., Vulpiani, G., Dietrich, S., 2019. The impact of lightning and radar reflectivity factor data assimilation on the very short-term rainfall forecasts of RAMS@ISAC: application to two case studies in Italy. Nat. Hazards Earth Syst. Sci. 19 (8), 1839–1864. https://doi.org/10.5194/nhess-19-1839-2019.
Federico, S., Torcasio, R.C., Puca, S., Vulpiani, G., Comellas Prat, A., Dietrich, S., Avolio, E., 2021. Impact of Radar Reflectivity and Lightning Data Assimilation on the Rainfall Forecast and Predictability of a Summer Convective Thunderstorm in Southern Italy. Atmosphere 12 (8), 958. https://doi.org/10.3390/atmos12080958.
Federico, S., Torcasio, R.C., Popova, J., Sokol, Z., Pop, L., Lagasio, M., Lynn, B.H., Puca, S., Dietrich, S., 2024. Improving the lightning forecast with the WRF model and lightning data assimilation: results of a two-seasons numerical experiment over Italy. Atmos. Res. 304, 107382. https://doi.org/10.1016/j.atmosres.2024.107382.
Ferrari, F., Maggioni, E., Perotto, A., Salerno, R., Giudici, M., 2023. Cascade sensitivity tests to model deep convective systems in complex orography with WRF. Atmos. Res., 106964 https://doi.org/10.1016/j.atmosres.2023.106964.
Fierro, A.O., Mansell, E.R., Ziegler, C.L., MacGorman, D.R., 2012. Application of a Lightning Data Assimilation Technique in the WRF-ARW Model at Cloud-Resolving Scales for the Tornado Outbreak of 24 May 2011. Mon. Weather Rev. 140 (8), 2609–2627. https://doi.org/10.1175/MWR-D-11-00299.1.
Forestieri, A., Lo Conti, F., Blenkinsop, S., Cannarozzo, M., Fowler, H.J., Noto, L.V., 2018. Regional frequency analysis of extreme rainfall in Sicily (Italy). Int. J. Climatol. 38 (S1). https://doi.org/10.1002/joc.5400.
Gallo, B.T., Clark, A.J., Dembek, S.R., 2016. Forecasting tornadoes using convection-permitting ensembles. Weather Forecast. 31, 273–295 doi: 10.1175/WAF-D- 15-0134.1.
Gascón, E., Laviola, S., Merino, A., Miglietta, M.M., 2016. Analysis of a localized flash-flood event over the Central Mediterranean. Atmos. Res. 182, 256–268. https://doi.org/10.1016/j.atmosres.2016.08.007.
Gastaldo, T., Poli, V., Marsigli, C., Cesari, D., Alberoni, P.P., Paccagnella, T., 2021. Assimilation of radar reflectivity volumes in a pre-operational framework. Quart. J. Royal Meteorol. Soc. 147 (735), 1031–1054. https://doi.org/10.1002/qj.3957.
Giazzi, M., Peressutti, G., Cerri, L., Fumi, M., Riva, I.F., Chini, A., Ferrari, G., Cioni, G., Franch, G., Tartari, G., Galbiati, F., Condemi, V., Ceppi, A., 2022. Meteonetwork: an open crowdsourced weather data system. Atmosphere 13 (6), 928. https://doi.org/10.3390/atmos13060928.
Gimhan, P.G.S., Neluwala, P., Acierto, R.A., 2023. High-resolution WRF simulations of a monsoon event (2019) over the Badulu Oya Catchment, Sri Lanka: role of cumulus parameterization condition and microphysics schemes. J. Earth Syst. Sci. 132, 166. https://doi.org/10.1007/s12040-023-02186-y.
Giorgi, F., 2006. Climate change hot-spots. Geophys. Res. Lett. 33 (8). https://doi.org/10.1029/2006GL025734.
Grams, J.S., Thompson, R.L., Snively, D.V., Prentice, J., Hodges, G.M., Reames, L.J., 2012. A climatology and comparison of parameters for significant tornado events in the United States. Weather Forecast. 27, 106–123. https://doi.org/10.1175/WAF-D-11-00008.1.
Groenemeijer, P., van Delden, A., 2007. Sounding-derived parameters associated with large hail and tornadoes in the Netherlands. Atmos. Res. 83, 473–487. https://doi.org/10.1016/j.atmosres.2005.08.006.
Grunwald, S., Brooks, H., 2011. Relationship between sounding derived parameters and the strength of tornadoes in Europe and the Usa from reanalysis data. Atmos. Res. 100, 479–488. https://doi.org/10.1016/j.atmosres.2010.11.011.
Hong, S.-Y., Noh, Y., Dudhia, J., 2006. A new vertical diffusion package with an explicit treatment of entrainment processes. Mon. Weather Rev. 134 (9), 2318–2341. https://doi.org/10.1175/MWR3199.1.
Hong, S.-Y., Noh, Y., Dudhia, J., 2012. Next-generation numerical weather prediction: Bridging parameterization, explicit clouds, and large eddies. B. Am. Meteorol. Soc. 93 (1). https://doi.org/10.1175/2011BAMS3224.1.
Hong, Song-You, Lim, Jeong-Ock Jade, 2006. The WRF single-moment 6-class microphysics scheme (WSM6). Asia-Pac. J. Atmos. Sci. 42 (2), 129–151.
Iacono, M.J., Mlawer, E.J., Clough, S.A., Morcrette, J., 2000. Impact of an improved longwave radiation model, RRTM, on the energy budget and thermodynamic properties of the NCAR community climate model. CCM3. J. Geophys. Res.: Atmos. 105 (D11), 14873–14890. https://doi.org/10.1029/2000JD900091.
Janjić, Z.I., 1994. The Step-Mountain Eta Coordinate Model: further Developments of the Convection, Viscous Sublayer, and Turbulence Closure Schemes. Mon. Weather Rev. 122 (5), 927–945. https://doi.org/10.1175/1520-0493(1994)122<0927:TSMECM>2.0.CO;2.
JPL MUR MEaSUREs Project, 2015. GHRSST Level 4 MUR Global Foundation Sea Surface Temperature Analysis. Ver. 4.1. PO.DAAC, CA, USA. Dataset accessed [2024-06-01] at. https://doi.org/10.5067/GHGMR-4FJ04.
Kain, J.S., 2004. The Kain–Fritsch convective parameterization: an update. J. Appl. Meteorol. 43 (1), 170–181. https://doi.org/10.1175/1520-0450(2004)043<0170:TKCPAU>2.0.CO;2.
Kain, J.S., Weiss, S.J., Bright, D.R., Baldwin, M.E., Levit, J.J., Carbin, G.W., Schwartz, C. S., Weisman, M.L., Droegemeier, K.K., Weber, D.B., Thomas, K.W., 2008. Some practical considerations regarding horizontal resolution in the first generation of operational convection-allowing NWP. Weather Forecast. 23 (5), 931–952. https://doi.org/10.1175/WAF2007106.1.
Keil, C., Heinlein, F., Craig, G.C., 2014. The convective adjustment time-scale as indicator of predictability of convective precipitation. Quart. J. Royal Meteorol. Soc. 140 (679), 480–490. https://doi.org/10.1002/qj.2143.
Lagasio, M., Parodi, A., Pulvirenti, L., Meroni, A., Boni, G., Pierdicca, N., Marzano, F., Luini, L., Venuti, G., Realini, E., Gatti, A., Tagliaferro, G., Barindelli, S., Monti Guarnieri, A., Goga, K., Terzo, O., Rucci, A., Passera, E., Kranzlmueller, D., Rommen, B., 2019. A synergistic use of a high-resolution numerical weather prediction model and high-resolution earth observation products to improve precipitation forecast. Remote Sens. 11 (20), 2387. https://doi.org/10.3390/rs11202387.
Lagasio, M., Campo, L., Milelli, M., Mazzarella, V., Poletti, M.L., Silvestro, F., Ferraris, L., Federico, S., Puca, S., Parodi, A., 2022. SWING, the Score-weighted improved

nowcasting algorithm: description and application. Water 14 (13), 2131. https://doi.org/10.3390/w14132131.
Lynn, B.H., Cohen, S., Druyan, L., Phillips, A.S., Shea, D., Krugliak, H.-Z., Khain, A.P., 2020. An examination of the impact of grid spacing on WRF simulations of wintertime precipitation in the mid-atlantic united states. Weather Forecast. 35 (6), 2317–2343. https://doi.org/10.1175/WAF-D-19-0154.1.
Maggioni, E.C., Manzoni, T., Perotto, A., Spada, F., Borroni, A., Giurato, M., Giudici, M., Ferrari, F., Zardi, D., Salerno, R., 2023. WRF data assimilation of weather stations and lightning data for a convective event in northern Italy. Bull. Atmos. Sci. Technol. 4 (1), 8. https://doi.org/10.1007/s42865-023-00061-8.
Maiello, I., Gentile, S., Ferretti, R., Baldini, L., Roberto, N., Picciotti, E., Alberoni, P.P., Marzano, F.S., 2017. Impact of multiple radar reflectivity data assimilation on the numerical simulation of a flash flood event during the HyMeX campaign. Hydrol. Earth Syst. Sci. 21 (11), 5459–5476. https://doi.org/10.5194/hess-21-5459-2017.
Mansell, E.R., Ziegler, C.L., MacGorman, D.R., 2007. A lightning data assimilation technique for mesoscale forecast models. Mon. Weather Rev. 135 (5), 1732–1748. https://doi.org/10.1175/MWR3387.1.
Marín, J.C., Barrett, B.S., Pozo, D., 2020. The tornadoes of 30–31 May 2019 in south-Central Chile: sensitivity to topography and SST. Atmos. Res. 249, 105301. https://doi.org/10.1016/j.atmosres.2020.105301.
Mastrangelo, D., Horvath, K., Riccio, A., Miglietta, M.M., 2011. Mechanisms for convection development in a long-lasting heavy precipitation event over southeastern Italy. Atmos. Res. 100 (4), 586–602. https://doi.org/10.1016/j.atmosres.2010.10.010.
Mazzarella, V., Maiello, I., Ferretti, R., Capozzi, V., Picciotti, E., Alberoni, P.P., Marzano, F.S., Budillon, G., 2020. Reflectivity and velocity radar data assimilation for two flash flood events in Central Italy: a comparison between 3D and 4D variational methods. Quart. J. Royal Meteorol. Soc. 146 (726), 348–366. https://doi.org/10.1002/qj.3679.
Mazzarella, V., Milelli, M., Lagasio, M., Federico, S., Torcasio, R.C., Biondi, R., Realini, E., Llasat, M.C., Rigo, T., Esbrí, L., Kerschbaum, M., Temme, M.-M., Gluchshenko, O., Parodi, A., 2022. Is an NWP-based nowcasting system suitable for aviation operations? Remote Sens. 14 (18), 4440. https://doi.org/10.3390/rs14184440.
Miglietta, M.M., Regano, A., 2008. An observational and numerical study of a flash-flood event over South-Eastern Italy. Nat. Hazards Earth Syst. Sci. 8 (6), 1417–1430. https://doi.org/10.5194/nhess-8-1417-2008.
Miglietta, M.M., Rotunno, R., 2016. An EF3 multivortex tornado over the ionian region: is it time for a dedicated warning system over Italy? Bull. Am. Meteorol. Soc. 97 (3), 337–344. https://doi.org/10.1175/BAMS-D-14-00227.1.
Miglietta, M.M., Mazon, J., Rotunno, R., 2017a. Numerical simulations of a tornadic supercell over the Mediterranean. Weather Forecast. 32 (3), 1209–1226. https://doi.org/10.1175/WAF-D-16-0223.1.
Miglietta, M.M., Mazon, J., Motola, V., Pasini, A., 2017b. Effect of a positive Sea Surface Temperature anomaly on a Mediterranean tornadic supercell. Sci. Rep. 7 (1), 12828. https://doi.org/10.1038/s41598-017-13170-0.
Petracca, M., Federico, S., Roberto, N., Puca, S., D'Adderio, L.P., Torcasio, R.C., Dietrich, S., 2024. A 13-year long strokes statistical analysis over the Central Mediterranean area. Atmos. Res. 304, 107368. https://doi.org/10.1016/j.atmosres.2024.107368.
Pleim, J.E., 2007. A combined local and nonlocal closure model for the atmospheric boundary layer. part I: model description and testing. J. Appl. Meteorol. Climatol. 46 (9), 1383–1395. https://doi.org/10.1175/JAM2539.1.
Rasmussen, E.N., Blanchard, D.O., 1998. A baseline climatology of sounding- derived supercell and tornado forecast parameters. Weather Forecast. 13, 1148–1164. https://doi.org/10.1175/1520-0434(1998)013<1148:ABCOSD>2.0.CO;2.
Ricchi, A., Miglietta, M.M., Bonaldo, D., Cioni, G., Rizza, U., Carniel, S., 2019. Multi-physics ensemble versus atmosphere–ocean coupled model simulations for a tropical-like cyclone in the Mediterranean Sea. Atmosphere 10 (4), 202. https://doi.org/10.3390/atmos10040202.
Ricchi, A., Sangelantoni, L., Redaelli, G., Mazzarella, V., Montopoli, M., Miglietta, M.M., et al., 2023. Impact of the SST and topography on the development of a large-hail storm event, on the Adriatic Sea. Atmos. Res. 296, 107078. https://doi.org/10.1016/j.atmosres.2023.107078.
Richard, E., Buzzi, A., Zängl, G., 2007. Quantitative precipitation forecasting in the Alps: the advances achieved by the mesoscale alpine programme. Q. J. R. Meteorol. Soc. 133 (625), 831–846. https://doi.org/10.1002/qj.65.
Roberts, N.M., Lean, H.W., 2008. Scale-selective verification of rainfall accumulations from high-resolution forecasts of convective events. Mon. Weather Rev. 136, 78–97.
Rodriguez, O., Bech, J., 2018. Sounding-derived parameters associated with tornadic storms in Catalonia. Int. J. Climatol. 38, 2400–2414 doi: 10.1002/joc.5343.
Schwartz, C.S., Kain, J.S., Weiss, S.J., Xue, M., Bright, D.R., Kong, F., Thomas, K.W., Levit, J.J., Coniglio, M.C., 2009. Next-day convection-allowing WRF model guidance: a second look at 2-km versus 4-km grid spacing. Mon. Weather Rev. 137 (10), 3351–3372. https://doi.org/10.1175/2009MWR2924.1.
Setvák, M., Lindsey, D.T., Novák, P., Wang, P.K., Radová, M., Kerkmann, J., Grasso, L., Su, S.-H., Rabin, R.M., Šťástka, J., Charvát, Z., 2010. Satellite-observed cold-ring-shaped features atop deep convective clouds. Atmos. Res. 97 (1–2), 80–96. https://doi.org/10.1016/j.atmosres.2010.03.009.
Skamarock, W.C., Klemp, J.B., Dudhia, J., Gill, D.O., Liu, Z., Berner, J., Wang, W., Powers, J.G., Duda, M.G., Barker, D.M., et al., 2019. A Description of the Advanced Research WRF, Version 4; No. NCAR/TN-556+STR, NCAR Technical Note. National Center for Atmospheric Research, Boulder, CO, USA, p. 145.
Sofokleous, I., Bruggeman, A., Michaelides, S., Hadjinicolaou, P., Zittis, G., Camera, C., 2021. Comprehensive methodology for the evaluation of high-resolution WRF multiphysics precipitation simulations for small, topographically complex domains. J. Hydrometeorol. 22 (5), 1169–1186. https://doi.org/10.1175/JHM-D-20-0110.1.
Solano-Farias, F., García-Valdecasas Ojeda, M., Donaire-Montaño, D., Rosa-Cánovas, J.J., Castro-Díez, Y., Esteban-Parra, M.J., Gámiz-Fortis, S.R., 2024. Assessment of physical schemes for WRF model in convection-permitting mode over southern Iberian Peninsula. Atmos. Res. 299, 107175. https://doi.org/10.1016/j.atmosres.2023.107175.
Stegehuis, A.I., Vautard, R., Ciais, P., Teuling, A.J., Miralles, D.G., Wild, M., 2015. An observation-constrained multi-physics WRF ensemble for simulating European mega heat waves. Geosci. Model Dev. 8 (7), 2285–2298. https://doi.org/10.5194/gmd-8-2285-2015.
Stensrud, D.J., Xue, M., Wicker, L.J., Kelleher, K.E., Foster, M.P., Schaefer, J.T., Schneider, R.S., Benjamin, S.G., Weygandt, S.S., Ferree, J.T., Tuell, J.P., 2009. Convective-scale warn-on-forecast system. Bull. Am. Meteorol. Soc. 90 (10), 1487–1500. https://doi.org/10.1175/2009BAMS2795.1.
Taszarek, M., Brooks, H.E., Czernecki, B., 2017. Sounding-derived parameters associated with convective hazards in Europe. Mon. Weather Rev. 145, 1511–1528. https://doi.org/10.1175/MWR-D-16-0384.1.
Taylor, K.E., 2001. Summarizing multiple aspects of model performance in a single diagram. J. Geophys. Res. Atmos. 106 (D7), 7183–7192. https://doi.org/10.1029/2000JD900719.
Tewari, M., N. C. A. R, et al., 2004. Implementation and verification of the unified NOAH land surface model in the WRF model (Formerly Paper Number 17.5). In: Proceedings of the 20th Conference on Weather Analysis and Forecasting/16th Conference on Numerical Weather Prediction, Seattle, WA, USA, Vol. 14.
Thompson, G., Field, P.R., Rasmussen, R.M., Hall, W.D., 2008. Explicit forecasts of winter precipitation using an improved bulk microphysics scheme. Part II: implementation of a new snow parameterization. Mon. Weather Rev. 136 (12), 5095–5115. https://doi.org/10.1175/2008MWR2387.1.
Thompson, R.L., Edwards, R., Mead, C.M., 2004. An update to the supercell composite and significant tornado parameters. In: Preprints, 22nd Conf. On Severe Local Storms, Hyannis, MA, P8.1. Amer. Meteor. Soc. Available online at: https://ams.confex.com/ams/pdfpapers/82100.pdf (last access 25 November 2024).
Torcasio, R.C., Federico, S., Puca, S., Vulpiani, G., Comellas Prat, A., Dietrich, S., 2020. Application of lightning data assimilation for the 10 October 2018 case study over Sardinia. Atmosphere 11 (5), 541. https://doi.org/10.3390/atmos11050541.
Torcasio, R.C., Papa, M., del Frate, F., Dietrich, S., Toffah, F.E., Federico, S., 2023a. Study of the intense Meteorological Event Occurred in September 2022 over the Marche Region with WRF Model: Impact of Lightning Data Assimilation on Rainfall and Lightning Prediction. Atmosphere 14 (7), 1152. https://doi.org/10.3390/atmos14071152.
Torcasio, R.C., Mascitelli, A., Realini, E., Barindelli, S., Tagliaferro, G., Puca, S., Dietrich, S., Federico, S., 2023b. The impact of global navigation satellite system (GNSS) zenith total delay data assimilation on the short-term precipitable water vapor and precipitation forecast over Italy using the Weather Research and forecasting (WRF) model. Nat. Hazards Earth Syst. Sci. 23 (11), 3319–3336. https://doi.org/10.5194/nhess-23-3319-2023.
Torcasio, R.C., Papa, M., del Frate, F., Mascitelli, A., Dietrich, S., Panegrossi, G., Federico, S., 2024. Data assimilation of satellite-derived rain rates estimated by neural network in convective environments: a study over Italy. Remote Sens. 16 (10), 1769. https://doi.org/10.3390/rs16101769.
UNDRR (United Nations Office for Disaster Risk Reduction and World Meteorological Organization), 2023. Global Status of Multi-Hazard Early Warning Systems. Geneva, Switzerland.
Wagner, A., Heinzeller, D., Wagner, S., Rummler, T., Kunstmann, H., 2018. Explicit convection and scale-aware cumulus parameterizations: high-resolution simulations over areas of different topography in Germany. Mon. Weather Rev. 146, 1925–1944. https://doi.org/10.1175/mwr-d-17-0238.1.
Wang, H., Sun, J., Fan, S., Huang, X.-Y., 2013. Indirect assimilation of radar reflectivity with WRF 3d-Var and its impact on prediction of four summertime convective events. J. Appl. Meteorol. Climatol. 52 (4), 889–902. https://doi.org/10.1175/JAMC-D-12-0120.1.
Weusthoff, T., Ament, F., Arpagaus, M., Rotach, M.W., 2010. Assessing the benefits of convection-permitting models by neighborhood verification: examples from MAP D-PHASE. Mon. Weather Rev. 138 (9), 3418–3433. https://doi.org/10.1175/2010MWR3380.1.
Wilks, D.S., 2006. Statistical Methods in the Atmospheric Sciences. Academic Press, London, p. 627.